4. Results and Discussions

Section A: Malathion Biodegradation

4.1 Bacterial identification

Microscopic observation reveled rod-shaped bacteria in isolates. All the isolates were motile and strained gram positive. They showed catalase, oxidase, motility, voges-proskauer, urease, and fermentation reaction and were devoid of methyl red and indole production activity. The laboratory biochemical test of microorganisms demonstrates the metabolic activity in terms of their growth specifications and enzymatic activity with the help of chemicals, bacterial medium, and nutrients to interpret noticeable transitions.

16S rRNA sequence analysis was performed for the identification 3 bacterial isolates. All isolates S_1, S_2 and S_4 showed 98 % similarity with the *Bacillus* sp. Nucleotide **s**equence analysis according with 16S-rRNA fragment and phylogenetic analysis with the help of MEGA program recognized *Bacillus* sp.S_1, *Bacillus* sp. S_2 and *Bacillus* sp.S_4 as the most dominating species. *Bacillus* sp. S_1 showed the close relationship with *Bacillus aryabhattai*, *Bacillus*. Sp. HC002, *Bacillus* megateriumetc. Similarly for *Bacillus* sp. S_2 and *Bacillus* sp. S_4 close relative's species were shown in **Figure 11**. *Bacillus* sp. of same kind was also identified by Adhikari *et al*. (2010) in the isolates obtained from sites contaminates with insecticides and pesticides including Malathion. Goda *et al.* (2010) reported isolation of five bacterial stains such as *Pseudomonas* sp., *Pseudomonas putida*, *Micrococcus lylae*, *Pseudomonas aureofaciens* and *Acetobacter liquefaciens* for Malathion degradation.

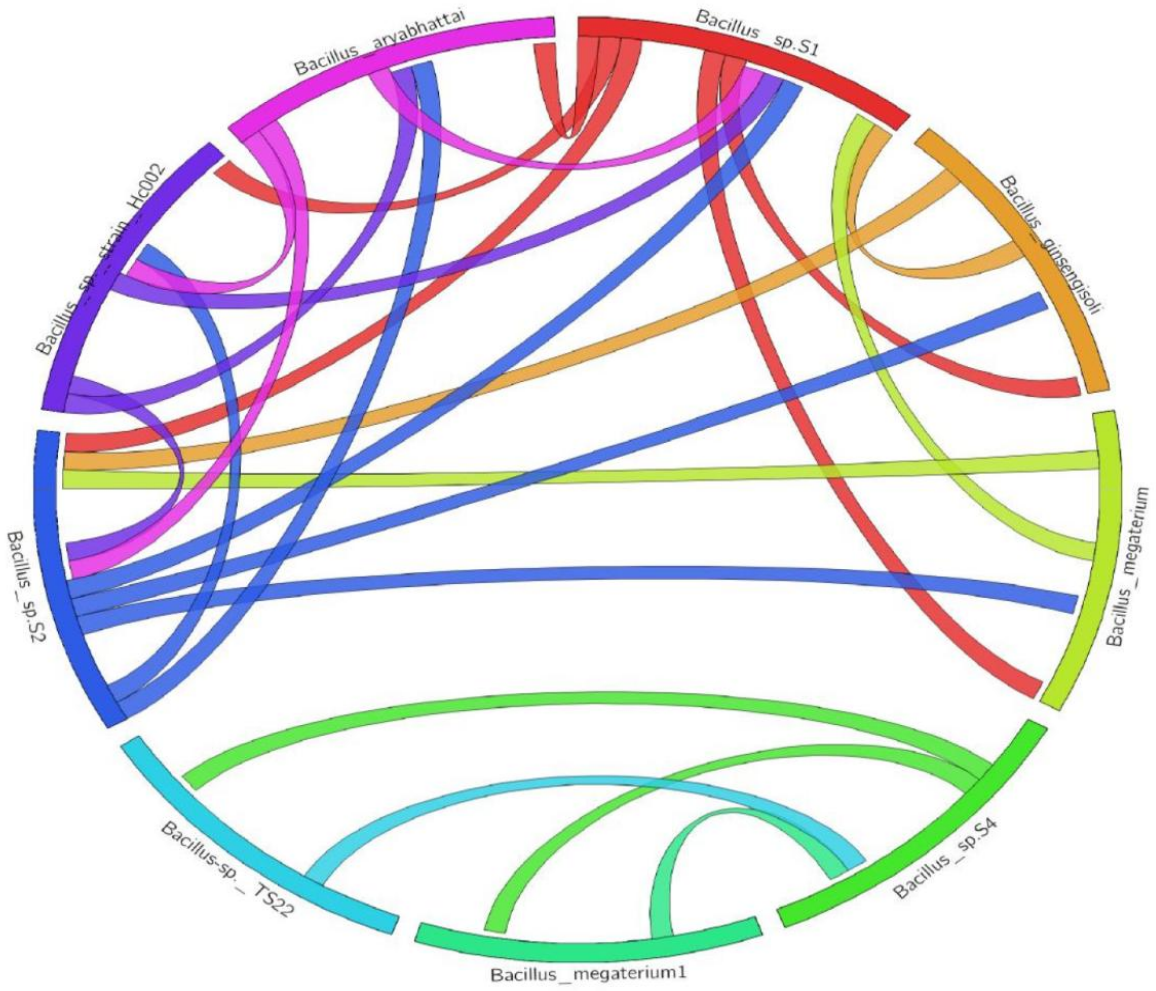

Figure 11: Circos visualization for *Bacillus* sp. S_1, *Bacillus* sp. S_2 and *Bacillus* sp. S_4

4.2 Selection of most efficient bacterial isolate

In the free cell experiments, the Malathion degradation capability of the three isolated species was analyzed in terms of average degradation rate with respect to Malathion concentration. The average degradation rate was increased upto concentration of 150, 175 and 200 mg/L of Malathion for *Bacillus* sp. S_1, S_2 and S_4 respectively and corresponding to these concentration the maximum average degradation rate was found to be 0.027, 0.031 and 0.0345per day (**Fig 12**).

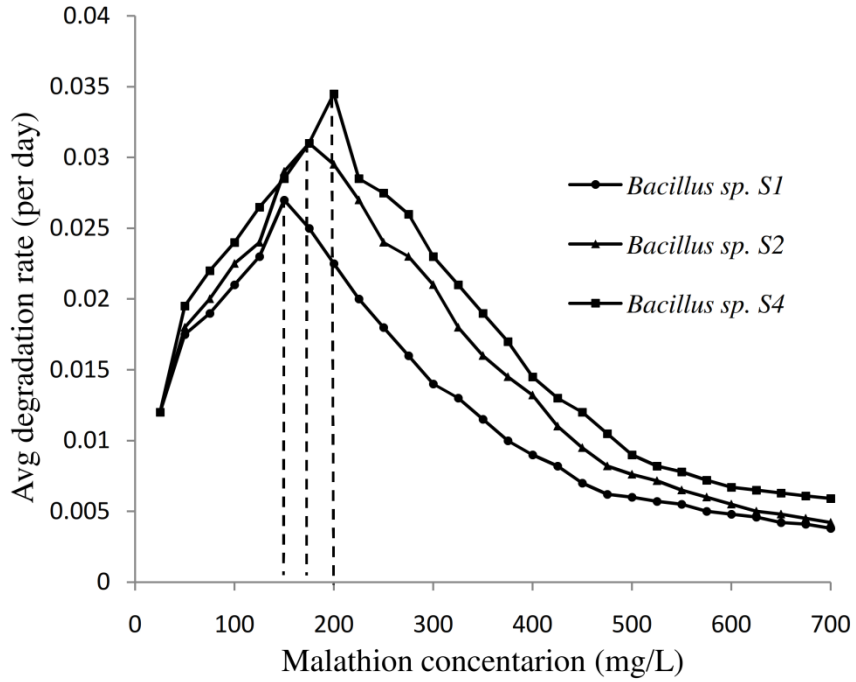

Figure 12: Average degradation rate (per day) of malathion by different isolated *Bacillus* species.

Decrease in average degradation rate beyond certain concentration is due to inhibitory effects of substrate on bacterial species (Azmy *et al*., 2015; Geed *et al*., 2016). The degradation was almost completed in 8 days and maximum degradation was obtained in case of *Bacillus* sp S_4 (**Fig 13**). The results confirmed the better efficacy of *Bacillus* sp. S_4 as compared to the other bacterial isolates in this study.

Further experimental trials were carried out by changing the concentration of Malathion from 25-700 mg/L in a free cell using *Bacillus* sp. S_4. Above 200 mg/L of Malathion, both removal and bacterial growth were found to be decreased which may be due to several reasons such as substrate inhibition, deficiency of nutrient and oxygen limitation. Similar results and trend were also obtained by Kim *et al*. (2005); Goda *et al*. (2010); Singh *et al*. (2012).

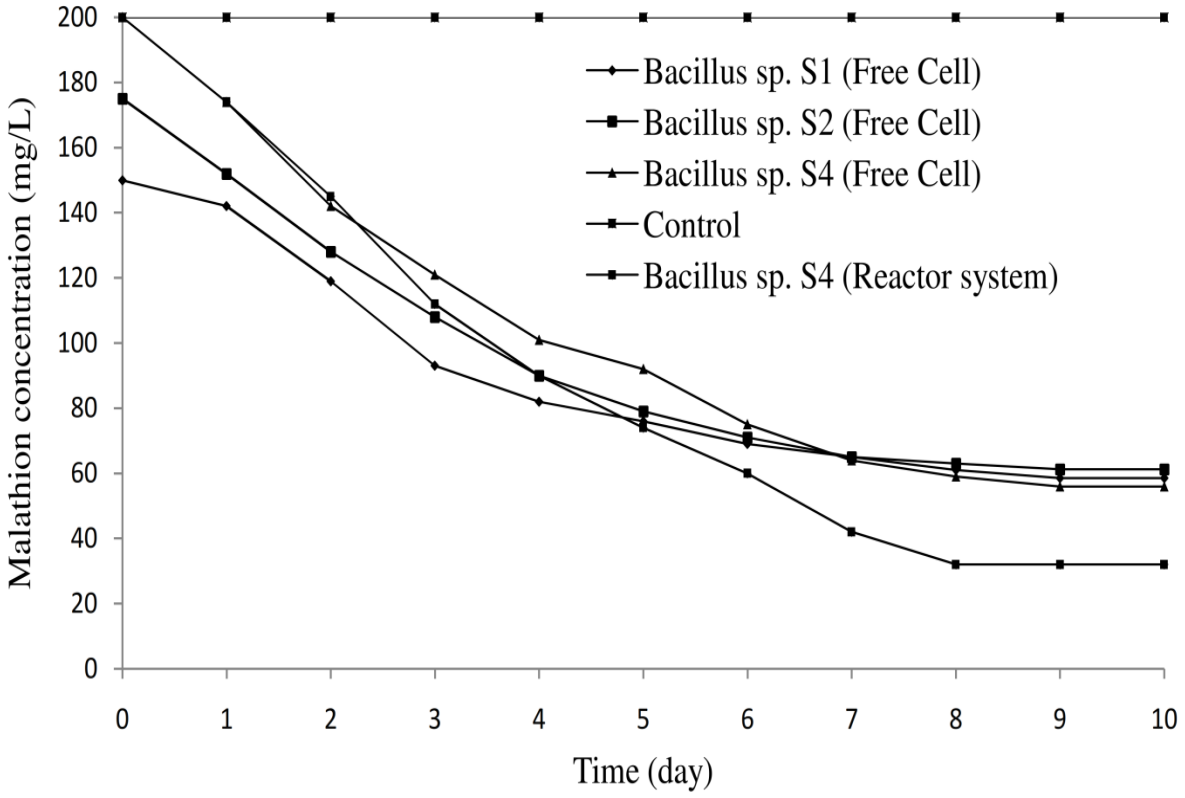

Figure 13: Removal of Malathion by *Bacillus* species in free and batch bioreactor system

4.3 Effect of pH and temperature in free cell system

The parametric optimization was performed using *Bacillus* sp. S_4 in free cell batch system at Malathion concentration of 200 mg/L. Degradation of malathion showed initial increasing trend with increase of pH from 5 and reached maxima of 71% at pH of 7.5. Thereafter a gradual decline in degradation was observed and it was limited to 52% at pH 10. The results showed that pH play a vital role during degradation of Malathion by enzymes released by microbial cells (Adhikari *et al*., 2010).

Effect of varying temperature (24^{o}C to 44^{o}C) on removal of Malathion was studied at fixed pH (7.5) and concentration (200 mg/L). There results indicated that highest percentage removal (72%) was achieved at 32^{o}C. Lowering of increasing the temperature lead to low

rate of malathion removal that may be attributed to effect of temperature on bacterial enzymatic activity. In nut shell, high and low temperature affects the enzymatic activity of the bacterium (Abdulsalam and Omale, 2009).

4.4 Biodegradation in packed batch bioreactor

The schematics of bioreactor is shown in **Figure 7** and **Table 4** packed with loofa sponge. Reactor was operated under the optimal conditions and optimized malathion concentration of 200 mg/L. After bacterial acclimatization of 20 days (acclimatization time), sufficient growth of *Bacillus* sp.S_4 (biofilm formation) took place on loofa as observed by SEM analysis shown in **Figure 14 (b)** and **Figure14 (c)**.

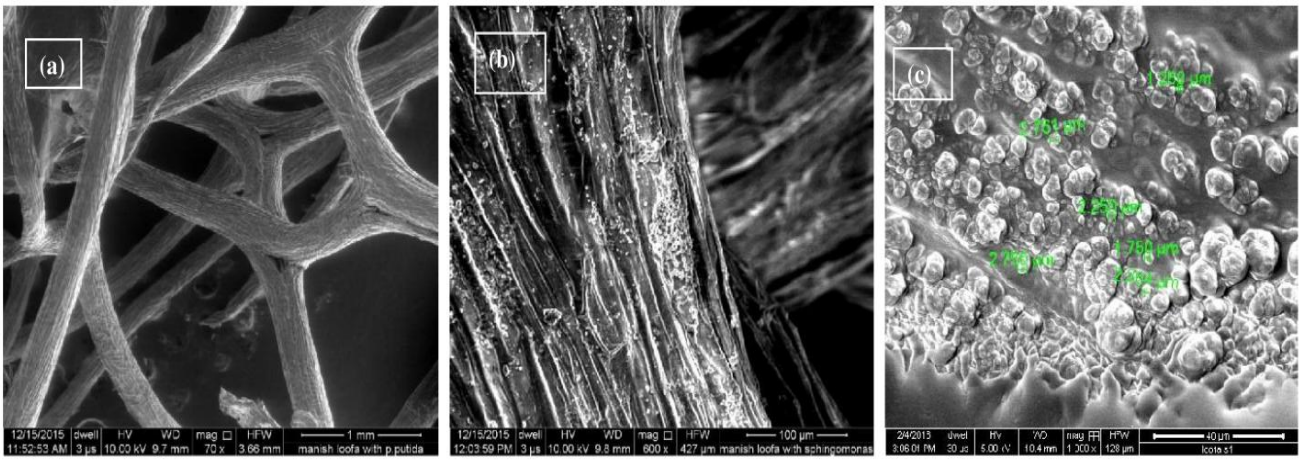

Figure 14: SEM images of (a) Loofa (b) Bacillus sp. S4 immobilized on loofa (c) Biofilm formed by Bacillus sp. S4 on loofa

In biodegradation experiments the removal of Malathion increased slowly and reached to 84% within 7^{th} days and it was better than free cell and bioreactor system as shown in **Figure 13**. The better performance of packed batch bioreactor may be due to several reasons such as more surface area available for growth of bacteria and its reaction with substrate (Singh *et al*., 2010; Yadav *et al*., 2014; Kureel *et al*., 2016; Geed *et al*., 2017), aeration in the

packed batch bioreactor which may result in homogeneous concentration and thus lesser possibility of channeling and formation of flogged biomass into the bioreactor (Kureel *et al*., 2017; Geed *et al*., 2017). Results in this current research showed improvement to the results reported by Singh *et al.* (2012) which showed 49.31% Malathion reduction by *Bacillus cereus* in a period of 7 days at 150 mg/L. In the present study, above 200 mg/L Malathion concentration, the % removal drops very swiftly which shows the probability of inhibition in the process. The higher residual concentration inside the reactor for the longer duration may result into adverse unfavorable condition in the bed and consequently lead to an inhibitory reaction on microbial biomass (Tazdait et al., 2013). They observed inhibitory effect on the growth of activated sludge (mix culture) beyond 140 mg/L Malathion concentration possibly due to toxicity exerted by Malathion and its metabolites.

4.5 Continuous PBBR: operation and performance estimation

During early stages of operation, the PBBR was supplied with 20 g/L glucose along with 10 mL inoculum specific to microorganism for growth of biofilm on the PUF. **Figures 15 (a)** and **(b)** show swift growth of microbial colonies on PUF and finally after 15 days a layer of biofilm was visible which explains complete immobilization. After completion of immobilization the operation of a continuous PBBR was started. Malathion degradation was investigated in continuous PBBR by changing feed rate from 5-30 mL/h (i.e., Malathion feeding rate) under the most favorable process parameters collected through the batch experiments. All the experiments were conducted at ambient temperature 33±5 °C.

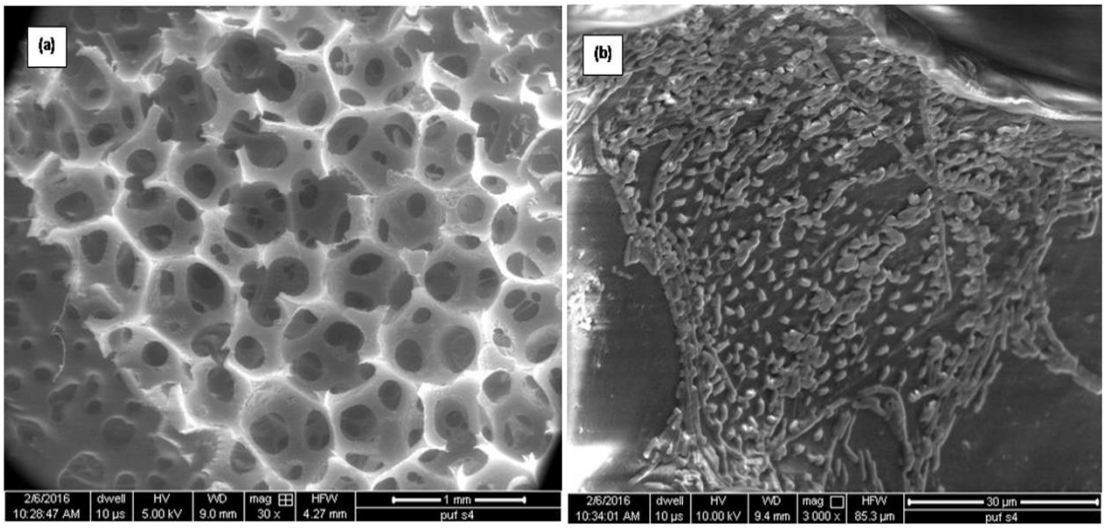

Figure 15: SEM images of *Bacillus Sp.*S_4 immobilized on PUF (a) PUF before immobilization (0 days) (b) immobilization after startup time (15^{th} day) of the packed bed bioreactor

Figure 15 also show the porous structure of PUF which is important in controlling large concentration of adhered biomass onto the exterior of PUF in the packed bed bioreactor which shows high rate of biodegradation.

Morphology of PUF in continuous PBBR facilitates more interaction with biomass and at the same time tend to decrease short circuiting and channeling of the hydrocarbon-laden stream leading to even distribution of malathion. Moussavi and Ghorebanian (2015) reported similar result for biodegradation of total petroleum hydrocarbon on PUF.

To check removal efficiency (RE) and elimination capacity (EC) of the reactor, 300 mg/L concentrated Malathion solution was continuously supplied for 15^{th} to 75^{th} day. Results are shown in **Figure 16** and **Table 5.** After the acclimation period (15 days) degradation of Malathion was operated in continuous packed bed bioreactor. Firstly, packed bed bioreactor was kept at a low feed rate (5 mL/h) of malathion analogous to inlet feeding rate of 36 mg/L/day to acclimate bacteria introduced into the biofilm for adaption to Malathion and to

begin the uniform condition (28th day). RE was observed to be almost 93 % while EC is 33.48 mg/L/day. During 30th day, the feed rate was changed to 10 mL/h corresponding to feeding rate of 72 mg/L/day. During the 31st day, a decline in RE was recorded but retrieved to stable value of 92% at end of 36th day while EC was measured to be 66.24 mg/L/day. Similar results were shown on 39th and 47th day when flow rate was changed to 15 and 20 mL/h respectively. During 56th day, flow rate was changed to 25 mL/h which is resulted in a decline of RE but retrieved and recorded to stable value of 80%. When the flow rate was changed to 30mL/h, a uniform % of RE was declined sharply and maintained at 67.33%.

Table 5: Different parameters for the performance of continuous packed bed bioreactor using *Bacillus sp.* S_4

Flow Rate (mL/h)	Operation Days	% RE Range	EC Range (mg/L/day)	Loading Rate (mg/L/day)
5	15-29	0-93	7.20-33.5	36
10	30-38	72-92	51.36-66.2	72
15	39-46	71.3-91.3	82.08-98.6	108
20	47-55	68-91	90.0-131.0	144
25	56-63	50-80	91.8-144.0	180
30	64-75	51-67.33	115.2-145.4	216

Analysis of variance was performed on various parameters to find the significance ($p<0.05$) on the degradation of Malathion. The value of standard deviation and standard deviation error was measured to be 18.61 and 2.40 for RE, 67.36 and 8.69 for inlet feeding rate and 44.89 and 5.79 mg/L·day for EC respectively (**Table 5**). Similar results were mentioned for wide range of pollutants (Yadav et al., 2014).

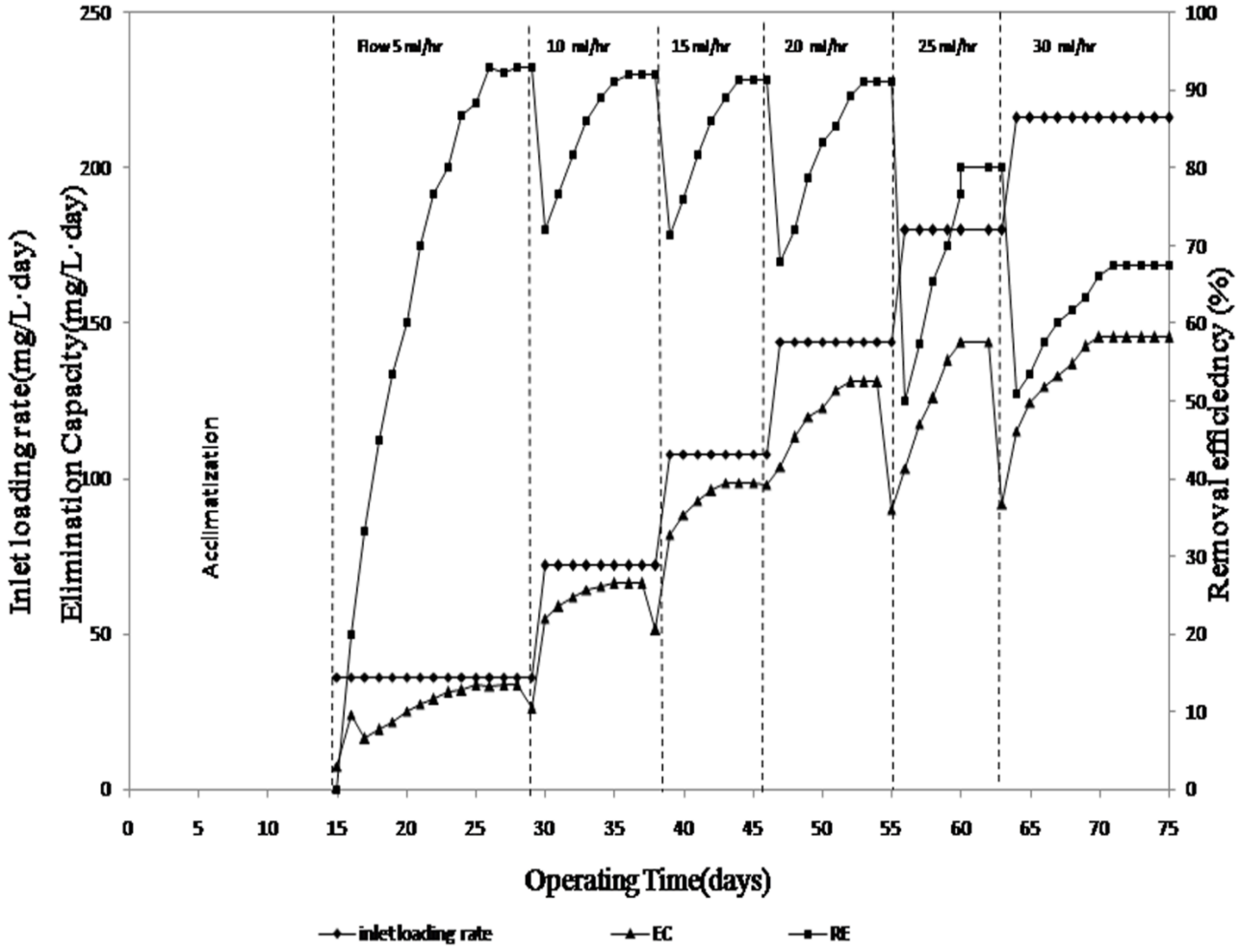

Figure 16: Effect of flow rate and inlet feed rate on degradation efficiency and elimination capacity for the performance of continuous PBBR

4.6 Effect of inlet loading rate, RE and EC for PBBR performance

Figure 17 shows the deviation of uniform EC and % RE with respect to the inlet feeding rate of Malathion. From the graph, we can conclude that RE is constant and EC follows a linear increase up to feeding rate 144 mg/L/day. Afterwards it is seen that RE commence to decrease while EC tends to a fixed value. This is the most pronounced fact debated by different researchers (Giri *et al*., 2015; Yadav *et al*., 2014) in view of rate controlling mechanisms in the reactor. In this condition when loading rate is 144 mg/L/day,

the rate controlling step of the reactor shift from the mass transfer to bio reaction. When the Malathion loading rate is higher and rate of hydrocarbons diffused into biomass (attached or biofilm) is below the critical rate gives way to MT (mass transfer) exceptions. High inlet loading of malathion leads to increased availability of hydrocarbon which results in to growth and expansion of biofilm. This intern causes increased surface area and availability of substrates, suitable to determination biodegradation kinetics. Hence, Malathion removal hinges on the capability of biomass to metabolize feasible substrate (Moussavi and Ghorebanian, 2015). Alternate facts that might lead to the decrease in RE is high feeding rate of bacteria plugging onto the surface of PUF and poor contact time among pollutant and enzyme substrate inhibition (Yadav *et al*., 2014).

The control zone for experimental operations, at inlet feeding rate of PBBR increases with decreasing RE at higher concentration of Malathion. The marked between RE percentage (85%) and EC (140 mg/L·day) curve is picked as proposed operating range of the reactorat inlet feed rate of 165 mg/L.day (**Fig. 17**). Yadav *et al*. (2014) has shown identical report and trends for pollutant Chloropyrifos by *Aspergillus sp.* as microorganisms.

Findings of the present study reveals the benefits of using solid support such as PUF including spongy complex for better water absorbing capability and increased adhesion among pollutant and microbes. Maximizing the contact time among micro-organisms and pollutants is a critical operational design for achieving optimum biodegradation performance (Friha *et al*., 2014; Moussavi and Ghorebanian, 2015). These packing materials also facilitated maximum rate of malathion degradation.

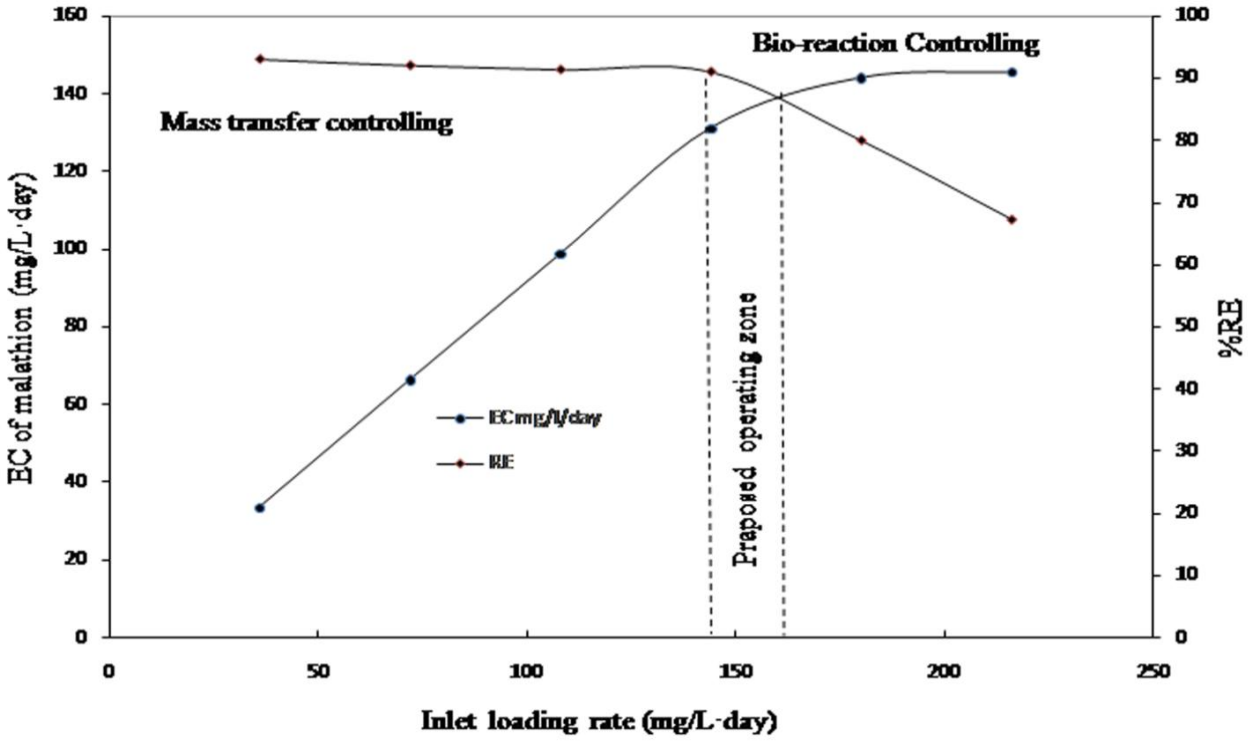

Figure 17: Correlation of proposed operating zone: Comparison among mass transfer controlling and bio-reaction controlling for the continuous PBBR

4.7 Analysis of metabolites: FTIR and GC/MS analysis

FTIR band spectrum of control Malathion without inoculum was found at the wave number 3228 per cm (**Fig 18**). FTIR spectrum of leachate confirms the presence of hydroxyl groups (-OH), carbonyl group (>C=O), –S- and –S–H– functional groups which clearly indicates the Malathion biodegradation and the results are similar to the findings of earlier publications (Srivastva *et al*., 2016; Giri and Pandey, 2013).

Further, GC/MS analysis was done to validate the FTIR results. In the GC/MS results, standard peak of pure Malathion ($C_{10}H_{19}O_6PS_2$) was observed at retention time of 18.191 min having molecular weight 330. The results of extracted leachate sample show the presence of diethyl mercaptosuccinate ($C_8H_{14}O_4S$), phosphorodithioic acid, O,O,S-trimethylester

($C_3H_9O_2PS_2$) at retention time of 12.547, 9.819 min and 206, 172 respectively. These are the stable metabolites produced during biodegradation of Malathion reported by other researchers (Janeczko *et al*., 2014).

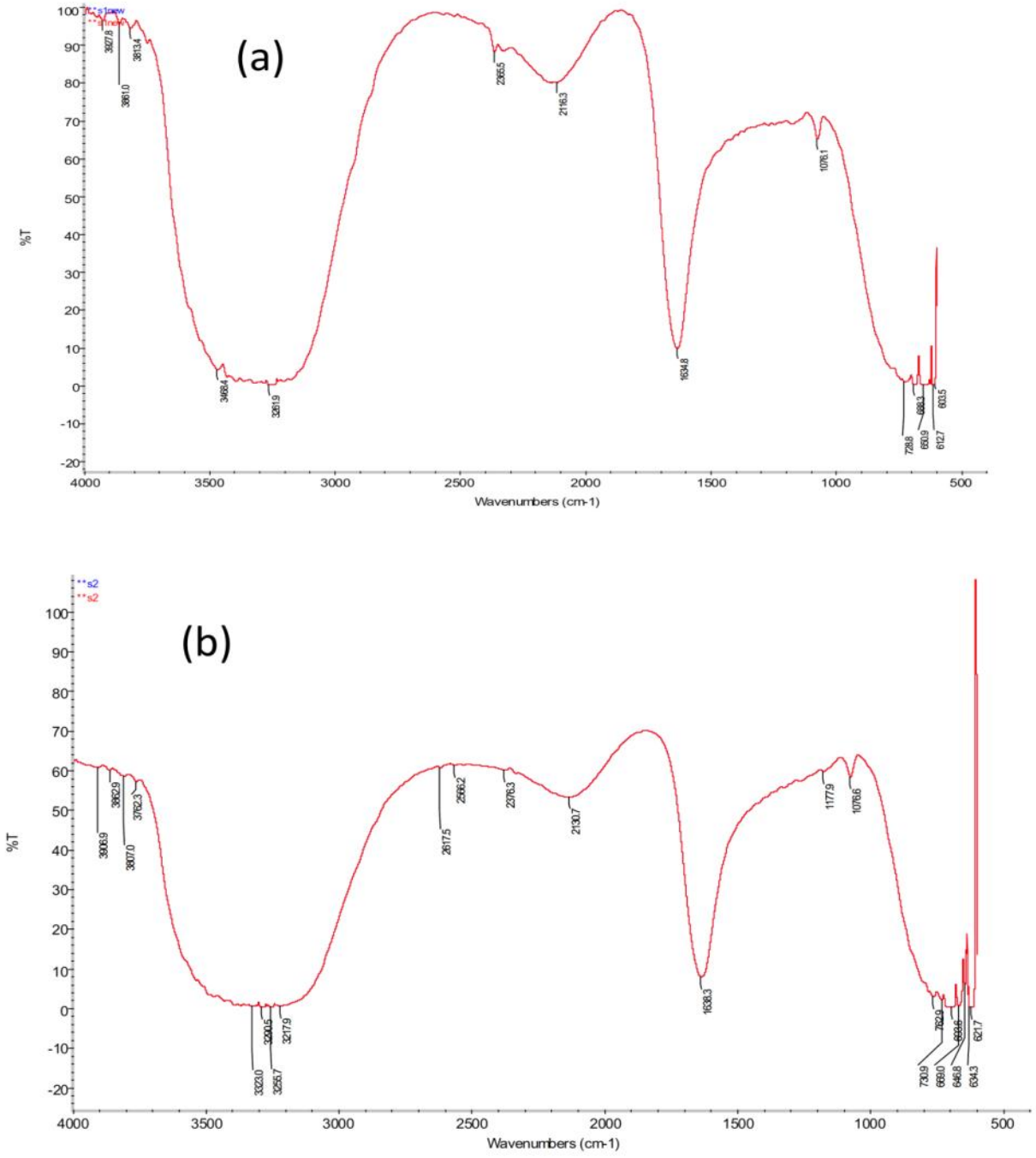

Figure 18: FT-IR results of (a) control Malathion sample and (b) after treatment

The GC-MS analysis was used to strengthen and confirm that Malathion biodegradation and metabolites formation as indicated by FT-IR results. Throughout the batch study, three tentative metabolites were observed using GC/MS library. These metabolites are namely malathion monocarboxylic acid, phosphorodithionicacid-O,O,S-trimethylester and succinic acid which are the biodegraded products of malathion. GC/MS analysis confirmed malathion degradation by *Bacillus* sp. S_4.The standard peak at m/z ratio 93, 125, 173,184, 256, 330 was observed These peaks indicated a parent ion peak of malathion (C10H19O6PS2) as shown in **Figure 19 (a)**. The parent ion goes through a transformation in the form of cleavage of –S-CH bond to produce two hugely abundant fragments, at m/z 173 and 125 respectively. The mass spectroscopy shows two new peaks at m/z 256 and 184 which indicates loss of –$COOC_2H_5$particles respectively, from the parent ion. The mass spectra in **Figure 19 (b)** reveals familiar features of Malathion monocarboxylic acid peak at m/z 93, 125, 158, 173 and 302. The **Figure 19(c)** and **(d)** shows the fragments of phosphorodithionic acid,O,O,S-trimethylester and succinic acid peak at m/z 93, 125, 172, 200 and peak at m/z 28, 56, 73, 100, respectively.

These conclusions proved Malathion degradation and malathion converting to three metabolites reported in this study which are in agreement with previously reported study (Singh *et al*., 2012; Janeczko *et al*, 2014).While some researchers have mentioned that hydrolysis of the ester bond is a frequent biodegradation step for organophosphorus compounds, it is not likely to be a vital part since the -P-S bonds were intact (Janeczko *et al*., 2014; Zhao and Hwang, 2009).Biodegradation is the disintegration of materials by bacteria, fungi, or other biological means takes place amid degradation of organic compounds. During Malathion biodegradation, stable and unstable intermediates are produced. The degradation

primarily relies on the kinds of enzymes or proteins liberated from bacteria to metabolize the organic compound (Janeczko *et al*., 2014). The detail of the biodegradation pathway was reported in previous publication Geed *et al*. (2017). Considering all the facts mentioned above, proteomic study was performed.

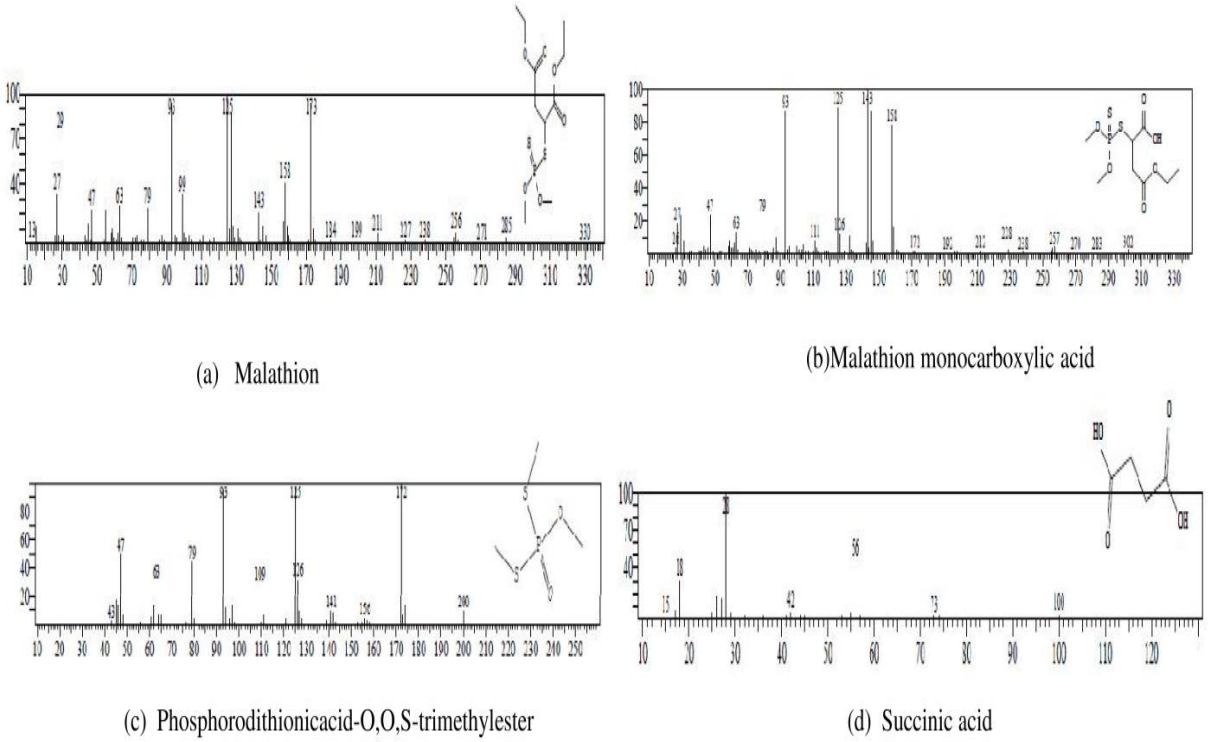

(a) Malathion

(b)Malathion monocarboxylic acid

(c) Phosphorodithionicacid-O,O,S-trimethylester

(d) Succinic acid

Figure 19: GC/MS analysis of (a) Malathion and metabolites (b) Malathion monocarboxylic acid, (c)Phosphorodithionicacid,O,O,S-trimethylester (d) Succinic acid.

4.8 Growth and inhibition kinetics

Monod and Andrew-Haldane models were applied to study the growth and inhibition kinetics of Malathion degradation by the isolated *Bacillus* species. Monod model was used for non inhibitory condition to estimate the kinetic parameters (μ_{max}, K_S and $\frac{\mu_{max}}{K_s}$) for all three species and measured to be 0.240/day, 132.48 mg/l and 0.001812 L/mg/day for *Bacillus* sp. S_1, 0.248 per day, 120 mg/L and 0.002067 L/mg/day for *Bacillus* sp. S_2 and 0.254 per

day, 119.5 mg/L and 0.002125 for *Bacillus sp.* S_4. Monod model fitted to the experimental data has been plotted as shown in **Figure 20 (a)** (Tomei *et al*., 2004; Yadav *et al*., 2014; Geed *et al.*, 2016; Srivastava *et al.*, 2016; Kureel *et al*., 2017). The value of $\frac{\mu_{max}}{K_s}$ simple quantitative parameter indicate the degradation ability of bacteria for particular pollutant. As expected and supported by other results, the value $\frac{\mu_{max}}{K_s}$ was found maximum for *Bacillus* sp. S_4.

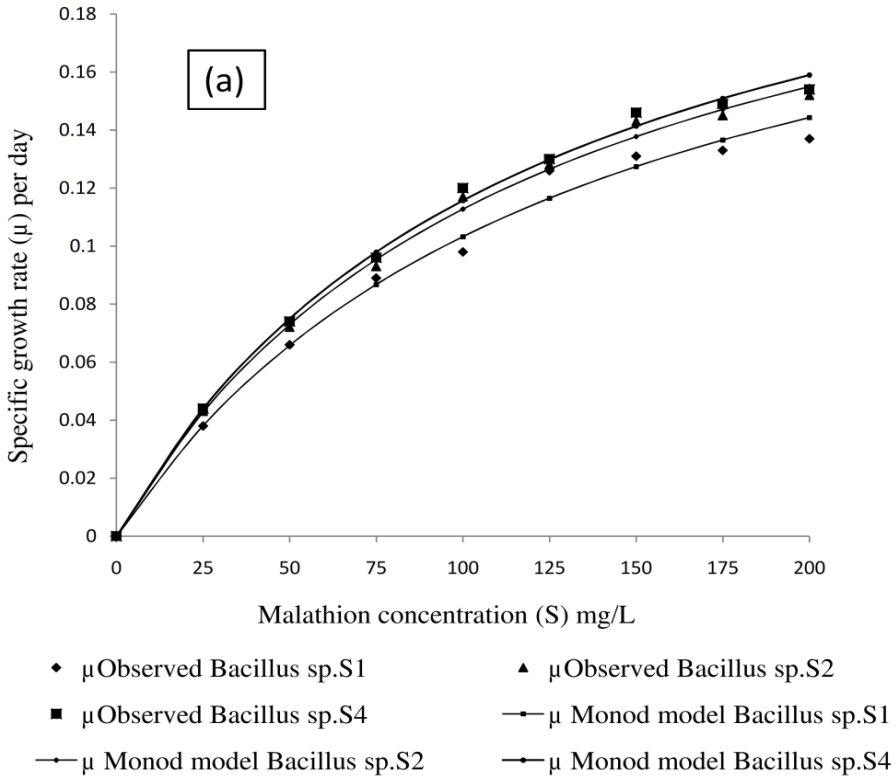

Figure 20 (a): Monod model growth kinetics for Malathion biodegradation

Under inhibitory conditions Andrew-Haldane growth inhibition kinetic model was taken to estimate kinetic parameters (μ_{max}, K_s and *Ki*) for all three species (**Figure 20b**). These parameters were measured to be 0.221/day, 122.03 mg/l, and 327.76 mg/L for *Bacillus* sp. S_1, 0.223 per day 115.91 mg/L, and 345.09 mg/L for *Bacillus* sp.$S_2$and 0.228/day, 114.8

mg/L and 348.43 mg/L for *Bacillus* sp. S_4. The value of $\frac{\mu_{max}}{K_s}$ again found higher for S_4. The value of Ki shows the Malathion concentration after which the inhibition will occur. This value also found maximum for S_4. Both results confirm that the *Bacillus* sp. S_4 has better potential to degrade Malathion as compared to other two species. The theoretically calculated Malathion concentration beyond which the inhibition will start were found more than experimentally calculated values (Shukla *et al.*, 2010; Kureel *et al.*, 2017; Geed *et al.*, 2017). The result indicated that there is possibility for further delay in inhibition and this may be obtained by optimization of process parameters. Limited reports are accessible on kinetic study of Malathion under inhibition and one of them is by Tazadait *et al* (2014) who studied inhibition kinetics for Malathion with changing concentration from 5 to 140 mg/L using Andrew-Haldane (Edwards 1970) inhibition model and mentioned that the values of K_s, μ_{max}, and K_i are 2318 mg/L, 2.96/hour and 2.718 mg/L respectively. The values of $\frac{\mu_{max}}{K_s}$ along with K_i are reported by Tazadait *et al* (2014) is significantly lower than all species isolated in this study which clearly indicate the great potential of all three bacterial species for Malathion degradation.

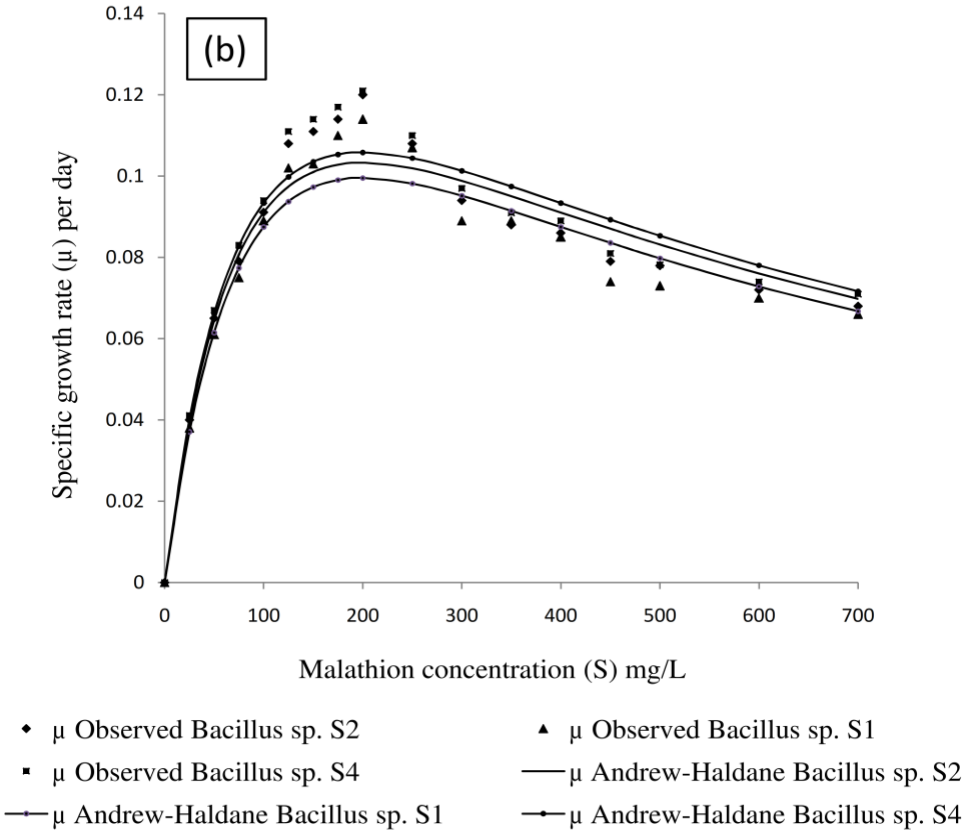

Figure 20 (b): Inhibition kinetics by Andrew-Haldane model for Malathion biodegradation

4.9 Proposed pathway: Malathion biodegradation

Biodegradation is the disintegration of organic compounds by bacteria, fungi, or other biological means. During the biodegradation, stable and unstable intermediates are produced. The route of biodegradation mainly relies on the kind of enzyme produced by bacteria to metabolize the organic compound. Different bacteria possess different biodegradation pathways for identical organic compounds. Limited studies are published on the biodegradation route of organic compounds containing Phosphorus moiety such as malathion. Despite the fact that some studies reported the hydrolysis of the ester bond As the standard biodegradation stage for organic compounds containing phosphorous, it is not expected to be an important mechanism because P-S bonds are intact (Janeczko *et al*., 2014;

Zhao and Hwang, 2009). Degradation route of mercaptosuccinate was examined and proposed by Konrad *et al.* (1969) show that diethyl succinate is broken down in the presence of desulfurization reaction with the help of enzymes such as diethyl succinate reductase to produce one mole of hydrogen sulfide and 2-mercapto succinic acid as byproduct. Another alternate pathway for biodegradation reported by Konrad *et al.* (1969) in which malathion was converted to phosphorous acid in a two stage reaction producing phosphorodithioic acid as a intermediate product using various kinds of enzyme such as dimethyl dithiophosphate-oxidoreductase, dimethyl thiophosphate- oxidoreductase sown in **Figure 21**.

Gas Chromatograph and Mass Spectroscopy analysis of separated leachate samples revealed the formation of 2 metabolites (mercaptosuccinate -$C_8H_{14}O_4S$; phosphorodithioic acid,O,O,S-trimethylester -$C_3H_9O_2PS_2$). These results along with FT-IR results were used to propose a biodegradation pathway for Malathion shown in **Figure 21**. Pathway of biodegradation of Malathion consists of two different protocols producing end products such as phosphorous, CO_2, H_2O and succinic acid. The first pathway is followed to produce succinic acid as final compound along with intermediates such as 2,2-thiodisuccinic acid. Two enzymes play a vital role in the first pathway where Malathion is converted to succinic acid using oxidoreductase enzyme (a). Thiosuccinate reductase enzyme (b) is produced by bacteria which converts 2, 2-thiosuccinic acid to diethyl mercaptosuccinate. Further, diethyl mercaptosuccinate reductase (c) is also produced by bacteria to convert diethyl mercaptosuccinate to 2-mercaptosuccinic acid and final product of succinic acid. Likewise, the second pathway culminates to produce phosphorous acid along with water and carbon dioxide. In the second route, three enzymes play vital role in conversion of Malathion to phosphoric acid. Oxidoreductase (x) is used to convert malathion into phosphorodithioic

acid,O,O,S-trimethyl ester and then to phosphorothionic acid by phosphodithioate phosphomonoesterase (y) enzyme produced by bacteria and finally to phosphoric acid using methylthiophosphate phosphomonoesterase (z) which is also produced by bacteria. Similar, pathway has been also reported by Janeczko *et al*. (2014) for biodegradation of Malathion with different parameters.

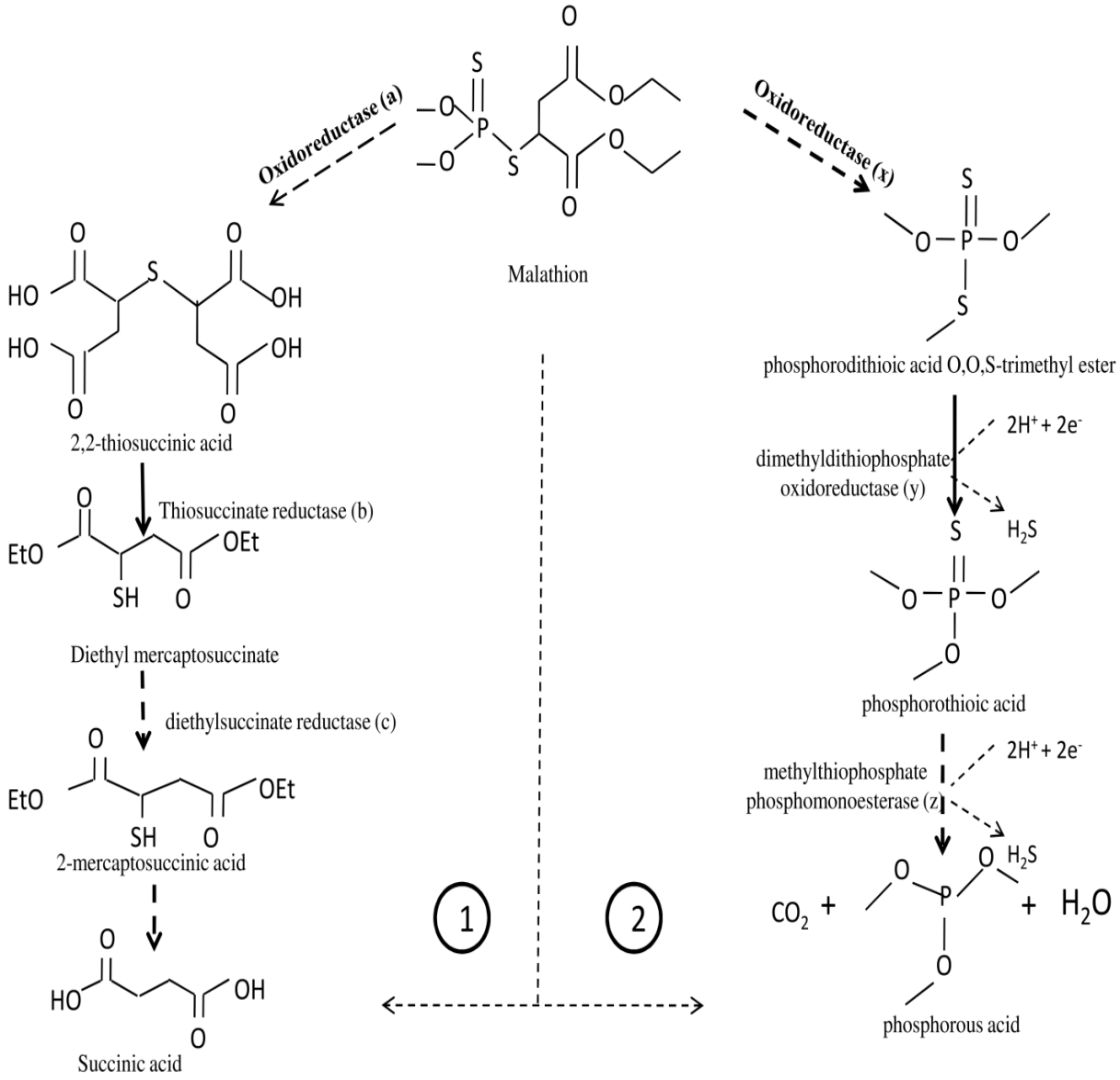

Figure 21: Proposed degradation pathway for Malathion

4.10 Proteomic analysis, spot identification and Maldi-Tof MS-MS Analysis

A sum of 395 protein spots were identified from control and treated gels using PD Quest™ basic version 8.0.1 in which 195 and 60 proteins spots were up and down accumulated respectively in treatment with respect to control. However 156 and 90 protein spots were unique between treatment and control. Furthermore 215 protein spots were common between these two Hence results of 2DE followed by PD-Quest analysis clearly demonstrated the variation in protein profile of the organism on treating with Malathion shown in **Figure 22**.

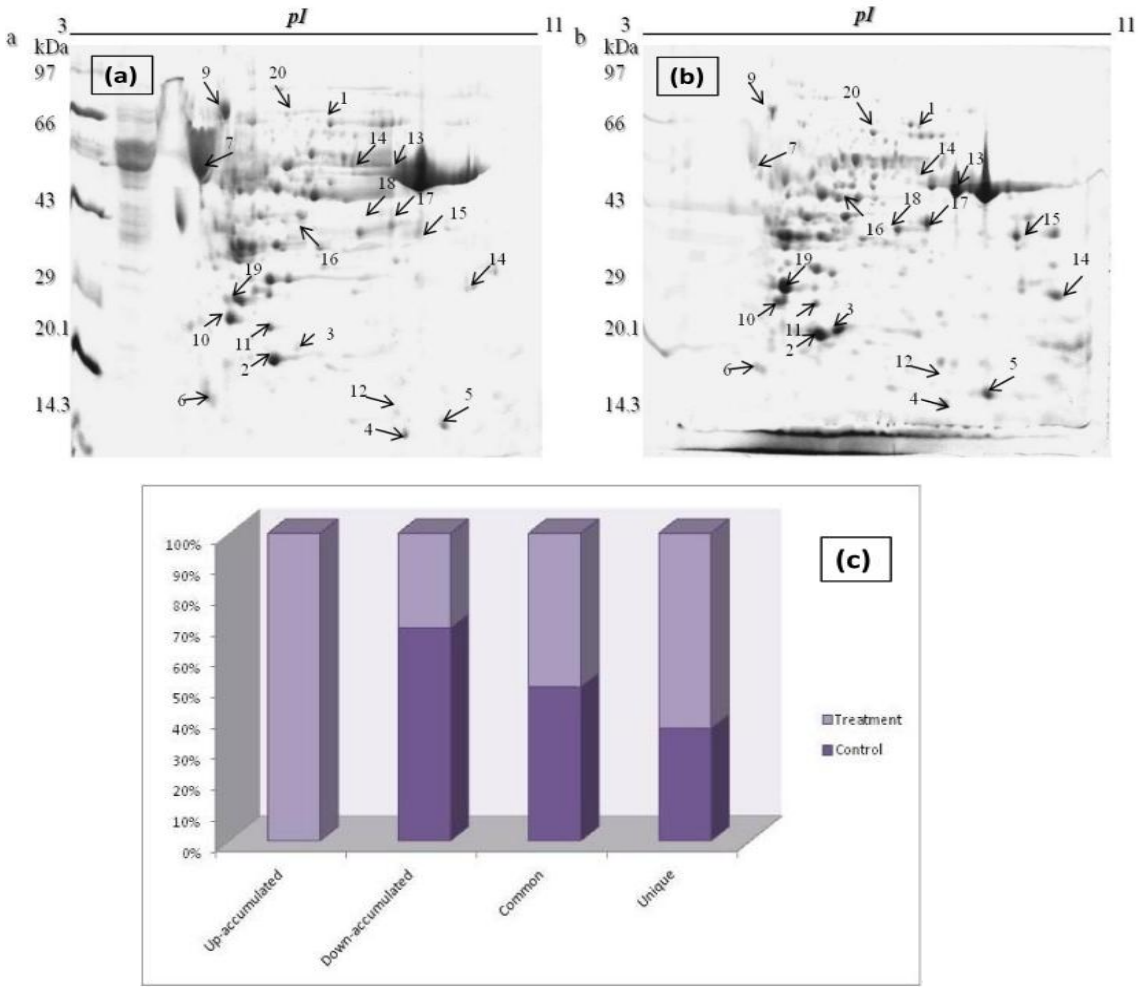

Figure 22: protein spot expressions of gel images

Molecular weight of many protein spots were revealed to be varying from 100 to 10 KDa and pH varying from 3 to 10. The results of 2DE perfectly demonstrate that there is significant change in the protein profile of *Bacillus* sp. on treating with Malathion. From (**Fig. 21**) 7 gel spots were chosen for MALDI-TOF-MS/MS analysis (3-control, 4-treated). Literature tells that protein spot must be identifiable as differentially specified proteins in the protein profile of well grown cells (*Bacillus* sp S_4).

4.11 *In silico* characterization of identified protein

4.11.1 Functional domain analysis, Phylogenic classification and Structural prediction

The 7 spots were successfully identified by MALDI-TOF analyses shown in **Table 6** in which 2 were hypothetical proteins having ID BAI87025.1 and NP_390682.1. In order to characterize proteins by functional, sequential and structural characterization *in-silico* analysis were performed using bioinformatics tools and server.

Table 6: MALDI-TOF analysis of protein

Spot .No.	Protein ID	Protein Name	Protein Sequence
		Control without malathion	
6.	NP_388753.1 *Bacillus* subtilis	Fe2+ or Zn2+ uptake regulation protein	MAAHELKEALETLKETGVRITPQRHAILEYLVNSMAHPTADDIYK ALEGKFPNMSVATVYNNLRVFRESGLVKELTYGDASSRFDFVTSD HYHAICENCGKIVDFHYPGLDEVEQLAAHVTGFKVSHHRLEIYGV CQECSKKENH
7.	ZP_06872829.1 *Bacillus* subtilis	Matrix biosynthesis Glycosyltransferases	MTKKILFCATVDYHFKAFHLPYFKWFKRMGWEVHVAASGQTKLP YVDEKFSIPIRRSPFHPQNLAVYRQLKEVIDTNQYDIVHCHTPVGG VLARLAARQARRHGTKVLYTAHGFHFCSGAPIKNWLLYYPVEKW LSAYTDCLITINEEDYIRAKGLQRPGGMTEKIHGIGVNTERFRPVSL QEKRNLREKHGFREDDFILVYPAELNLNKNQKLLIEAAALLKENIP SLRLVFAGEGAMEQAYRMLAEKLGASGNVRFYGFCRDIHELIQLA DVSVASSIREGLGMNVLEGMAAEKPAIATDNRGHREIIRDGENGFL IKIGDSAAFACRIEQLYHKPELCKKLGQEGRKTALRFSESRTVEEM ADIYSAYMDMDTKEKSV
10.	BAI87025.1	Hypothetical protein BSNT_10000	MKYKQIKTKKIYEEVADALLDMIKNGELKPGDKLDSVQALAESFQ VSRSAVREALSALKAMGLVEMKQGEGTYLKEFELNQISQPLSAAL LMKKEDVKQLLEVRKLLEIGVASLAAEKRTEADLKRIHDALKEM GSIEADGELGEKADFAFHLALADASQNELLKHLMNHVSSLLLETM RETRKIWLFSKKTSVQRLYEEHERIYNAVAAGNGAQAEAAMLAH LTNVEDVLSGYFEENVQ

Treated with malathion			
4.	ZP_06873063.1 *Bacillus* subtilis	Helix-turn-helix XRE-family like proteins	MFDLKEFGCLLQKIRKKRKMSQIEFAQLLGFTASYVSRVERGKAN PSIQAIEKITKQLNIKIRIFFD
11.	NP_390682.1	Hypothetical protein BSU28040	MVIHDLPLKLKDFPMKEKPRERLLKVGAENLANHELLAILLRTGT KHESVLDLSNRLLRSFDGLRLLKEASVEELSSIPGIGMVKAIQILAA VELGSRIHKLANEEHFVIRSPEDGANLVMEDMRFLTQEHFVCLYL NTKNQVIHKRTVFIGSLNSSIVHPREVFKEAFKRSAASFICVHNHPS GDPTPSREDIEVTRRLFECGNLIGIELLDHLVIGDKKFVSLKEKGYL
19	KFF56506.1	GroEL	MAKDIKFSEEARRAMLRGVDALADAVKVTLGPKGRNVVLEKKFG SPLITNDGVTIAKEIELEDAFENMGAKLVAEVASKTNDVAGDGTTT ATVLAQAMIREGLKNVTAGANPVGVRKGMEQAVAVAIENLKEIS KPIEGKESIAQVAAISAADEEVGSLIAEAMERVGNDGVITIEESKGF TTELEVVEGMQFDRGYASPYMVTDSDKMEAVLDNPYILITDKKIT NIQEILPVLEQVVQQGKPLLLIAEDVEGEALATLVVNKLRGTFNAV AVKAPGFGDRRKAMLEDIAVLTGGEVITEDLGLDLKSTQIAQLGR ASKVVVTKENTTIVEGAGETDKISARVTQIRAQVEETTSEFDREKL QERLAKLAGGVAVIKVGAATETELKERKLRIEDALNSTRAAVEEGI VSGGGTALVNVYNKVAAVEAEGDAQTGINIVLRALEEPIRQIAHN AGLEGSVIVERLKNEEIGVGFNAATGEWVNMIEKGIVDPTKVTRS ALQNAASVAAMLLTTEAVVADKPEENAGGAGMPDMGGMGGMG GMM
9	CAA70643.1	YisO	MTDTLSKRGPDDSNVWGEHHVLFGHKRLAVVDIEGGRQPMACTY KGDTYTIIYNGELYNTEDLRKELRAR GHQFERTSDTEVLLHSYIEWQEDCVDHLNGIFAFAVWDEKRNLLF AARDRLGVKPFFYTKEGSSFLFGSE IKAILAHPDIKARVDRTGLSEIFGLGPSRTPGTGIFKGIKEIRPAHALT FSKDGLNIWRYWNVESEKHTD SFDDTVANVRSLFQDAVTRQLVSDVPVCTFLSGGLDSSAITAIAAG HFEKEGKAPLHTYSIDYEENDKYF QASAFQPNDDGPWIEKMTEAFGTTHHKCVISQKDLVDHLEEAVLV KDLPGMADVDSSLLWFCREIKKDFV VSLSGECADEIFGGYPWFHTADVESGFPWMRSTEERIKLLSDSWQ KKLNLKEYVNAKYEETLAETPLLDG ETGVDKARRQLFYLNMLWFMTNLLDRKDRMSMGASLEVRVPFA DHRLVEYVWNIPWEMKMHDNREKGILR KALEGILPDDILYRKKSPYPKTHHPEYTKGVSEWLKTIRSQKDSVL HTLLDRKQLDQLLETEGSSFKVPW FGQLMKGPQLIAHLAQIHTWFEAYRIDIDER

PFAM server was used to study their functional domain, detail are given in **Table 7**. The 5 known characterized identified proteins were Fe^{2+} or Zn^{2+} uptake regulation protein (NP_388753.1), putative extracellular matrix biosynthesis protein (ZP_06872829.1), XRE family protein (ZP_06873063.1), GroEL (KFF56506.1) and YisO (CAA70643.1). NP_388753.1 is a Ferric uptake regulator family protein with PFAM No.(PF01475) involved in iron uptake (Fur) and peroxide regulon (PerR) repressors and zinc-specific metal ore regulatory protein controlling zinc transport operons in *Bacillus subtilis* (Bsat *et al*., 1998;

Gaballa and Helmann, 1998). ZP_06872829.1 is putative extracellular matrix biosynthesis protein is Glycosyltransferases group family protein having PF00534 plays structural and functional role (Vetting *et al*., 2008). ZP_06873063.1XRE-family like proteins (PF01381) having important role as operator-binding domain of lambda repressor in structure and DNA recognition (Pabo and Lewis, 1982). KFF56506.1 (GroEL) is a TCP-1/cpn60 chaperonin family protein with PFAM No. (PF00118) which shows bifunctional role in genetics and development also showed development of crystal structure in bacterial chaperonin (Braig *et al*., 1994; Kaufman, 2003).YisO (CAA70643.1) is glutamine amidotransferase domain family protein (PF13537) showed important function in asparagine synthetase genes of *Bacillus subtilis* (Yoshida *et al*., 1991). The details of the functional role are given in **Table 7.**

The other 2 spots identified as hypothetical proteins, were characterized by (INTERPROSCAN, PROSITE, CDD AND PFAM) server. The hypothetical protein (BAI87025.1) is a GntR bacterial regulatory protein with GntR family (PF00392) have major role in plasmid maintenance in *Anabaena* sp. (Lee *et al.*, 2003) and role of fatty acid-responsive transcription factor for coenzyme fold binding (Van-Aalten *et al.*, 2000). Another hypothetical protein (NP_390682.1) is a most dominant predicted protein with treated Malathion used for docking. This protein is a Helix-hairpin-helix motif family protein with (PF00633) plays important role in DNA-binding and DNA repairing (Doherty *et al*., 1996; Rafferty *et al*., 1996; Denver *et al*., 2003). The detail of the functional role of identified hypothetical protein is given in **Table 7**.

Table 7: Functional domain details of identified proteins

S.N.	Protein ID	Protein Name	Interproscan; Prosite; CDD; SMART; Pfam	References
9.	NP_388753.1 *Bacillus* subtilis	Fe2+ or Zn2+ uptake regulation protein	FUR; (PF01475) Ferric uptake regulator family	Bsat et al. (1998); Gaballa and Helmann (1998)
10.	ZP_06872829.1 *Bacillus* subtilis	Glycosyltransferases	Glycosyltransferases group 1 (PF00534); Glycosyltransferase Family 4 (PF13439)	Vetting et al. (2008)
12.	BAI87025.1	hypothetical protein BSNT_10000	GntR; (PF00392); Bacterial regulatory proteins, gntR family	Lee et al. (2003) ;Van-Aalten et al. (2000)
			FCD; (PF07729); FCD domain	Van-Aalten et al. (2000)
11.	ZP_06873063.1 *Bacillus* subtilis	Helix-turn-helix XRE-family like proteins	HTH_XRE; (PF01381); Helix-turn-helix	Vetting et al. (2008)
13.	NP_390682.1	hypothetical protein BSU28040	HHH; (PF00633); Helix-hairpin-helix DNA-binding	Gaballa and Helmann (1998)
15	KFF56506.1	molecular chaperone GroEL	Cpn60_TCP1 ; (PF00118); TCP-1/cpn60 chaperonin family	Lee et al. (2003)
16	CAA70643.1	YisO	GATase_7; (PF13537); Glutamine amidotransferase domain	Yoshida et al. (1999)

The sequential classification was performed by phylogenetic analysis for characterized protein with similar or closely related species to *Bacillus cereus* shown in **Figure 23**.

Sequential classification revealed the proper clustering along with *Bacillus cereus* and tree construction were performed by MEGA6 software (**Figure 23**).

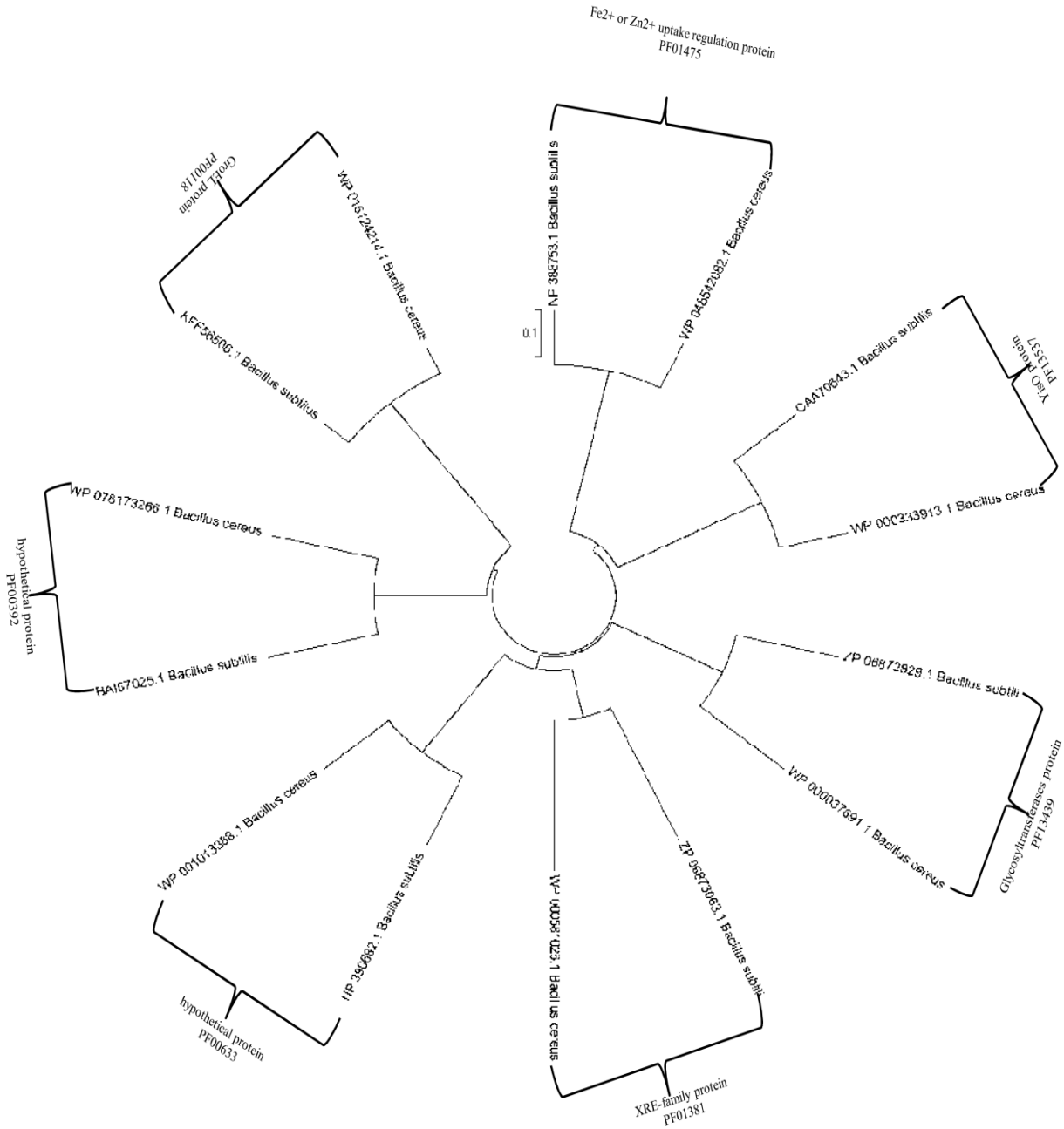

Figure 23: Phylogenic analysis and functional details (PFAM no) of identified characterized protein with similar or closely related reference species

Structural prediction and analysis were performed using discovery studio and Swiss model server. The best contracted structure was taken for docking analysis. The details of RAMPAGE statistics were reported in **Table 8(a)** and **Table 8(b)** obtained from RAMPAGE server. From RAMPAGE table the 3D structure of identified protein with best quality was given in **Figure 24** and other 3D-structure are shown in **Figure 25**.

Table 8 (a): Quality assessment of protein structure models obtained by Discovery Model

Accession No.	**Protein Name**	**Number of residues in favored region (~98.0% expected)**	**Number of residues in allowed region (~2.0% expected)**	**Number of residues in outlier region**
NP_388753.1	9. peroxide operon regulator [*Bacillus* subtilis]	97.2%	1.4%	1.4%
ZP_06872829.1	10. putative extracellular matrix biosynthesis enzyme [*Bacillus* subtilis]	90.4%	8.0%	1.6%
BAI87025.1	12. hypothetical protein [*Bacillus* subtilis]	98.6%	0.0%	1.4%
ZP_06873063.1	11. XRE family protein [*Bacillus* subtilis]	96.9%	3.1%	0.0%
NP_390682.1	13. hypothetical protein [*Bacillus* subtilis]	98.0%	2.0%	0.0%
KFF56506.1	15. GroEL [*Bacillus* subtilis]	98.4%	1.2%	0.5%
CAA70643.1	16. YisO [*Bacillus* subtilis]	-	-	-

Table 8(b): Quality assessment of protein structure models obtained by Swiss Model

Accession No.	Protein Name	Number of residues in favored region (~98.0% expected)	Number of residues in allowed region (~2.0% expected)	Number of residues in outlier region
NP_388753.1	9. peroxide operon regulator[*Bacillus* subtilis]	80.0%	11.9%	8.1%
ZP_06872829.1	10. putative extracellular matrix biosynthesis enzyme [*Bacillus* subtilis]	92.6%	6.3%	1.1%
BAI87025.1	12. hypothetical protein[*Bacillus* subtilis]	98.2%	1.8%	0.0%
ZP_06873063.1	11. XRE family protein[*Bacillus* subtilis]	100.0%	0.0%	0.0%
NP_390682.1	13. hypothetical protein[*Bacillus* subtilis]	86.0%	10.8%	3.2%
KFF56506.1	15. GroEL [*Bacillus* subtilis]	93.8%	5.6%	0.6%
CAA70643.1	16. YisO [*Bacillus* subtilis]	89.6%	7.7%	2.7%

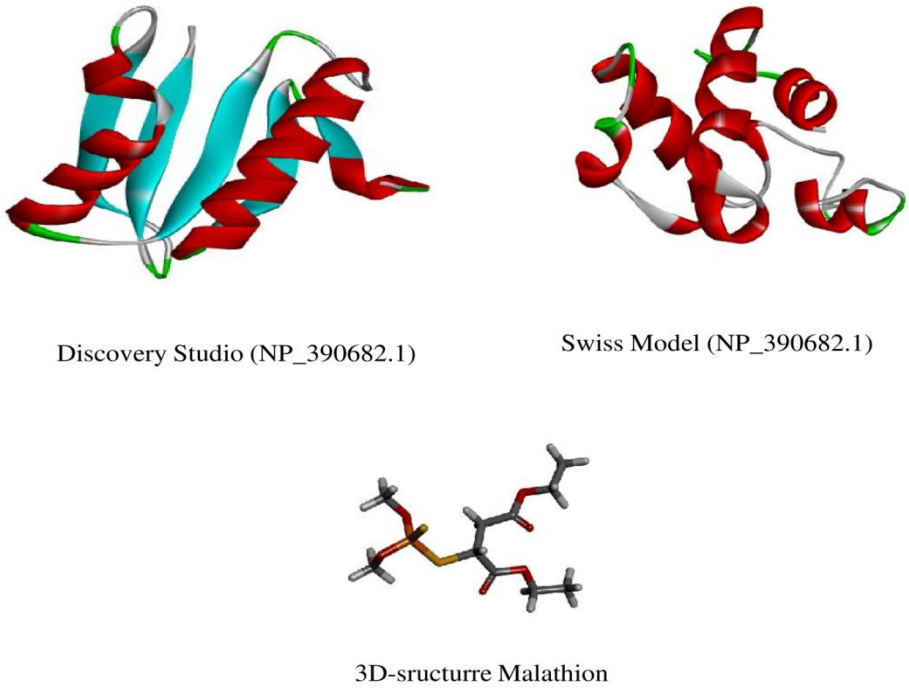

Figure 24:3D Structure of hypothetical protein (NP_390682.1) by Discovery Studio and Swiss Model and Malathion drug used for molecular docking

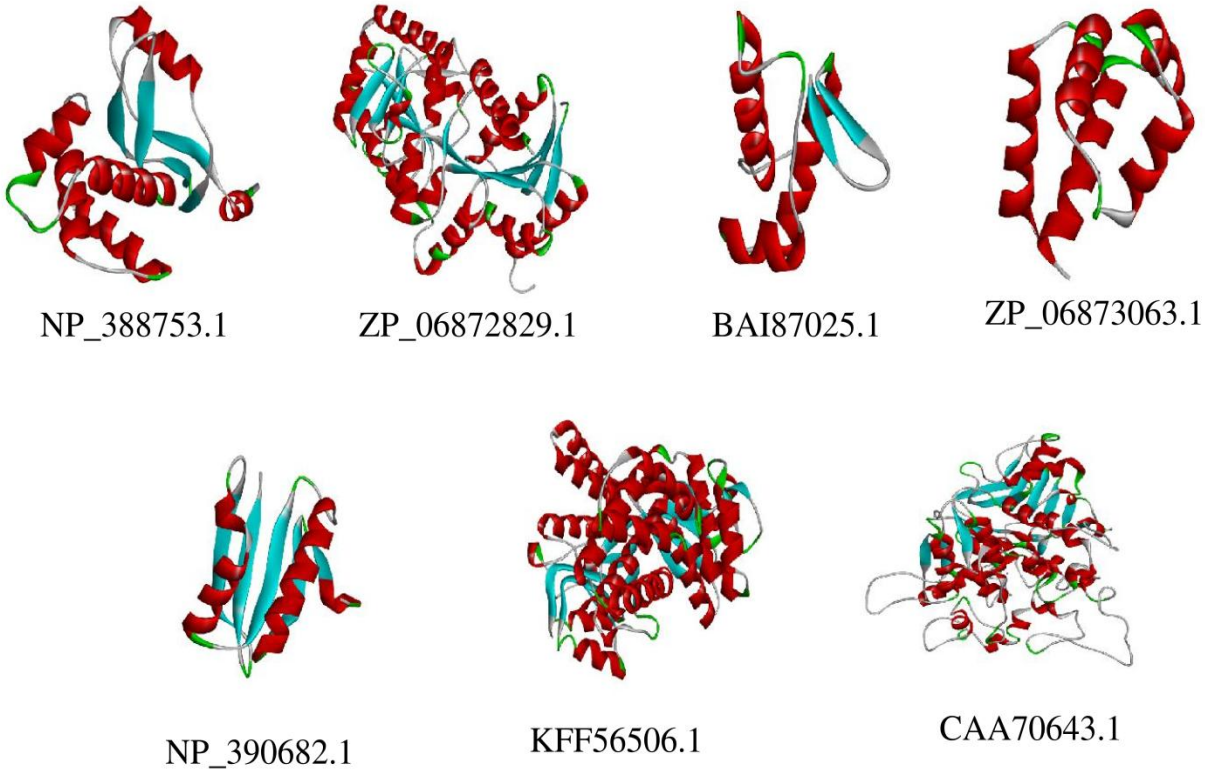

Figure 25: The 3D structures of identified protein

4.11.2 Molecular docking and active site analysis

The best predicted model (NP_390682.1) from **Table 8 (a)** and **Table 8 (b)** was selected (treated with Malathion pesticide) as reliable structure as shown in **Figure 24** and used for docking calculation. The major active binding sites were predicted using Meta pocket server shown in **Table 9**.

Table 9: Major active binding site and residues

Major active binding sites	Active binding residues
Active binding sites 1	HIS^{182}, SER^{190}, ASP^{193}, GLU^{130}, ASN^{181} PRO^{183}, PRO^{189}, GLU^{192}, HIS^{180}, HIS^{131} HIS^{214}, ILE^{151}, VAL^{196}, VAL^{159}, GLY^{152} PHE^{132}, SER^{153}, GLU^{195}, SER^{156}, LEU^{200} ASN^{155}, PHE^{150}, LEU^{154}, ARG^{199}, PRO^{161} ILE^{158}, HIS^{160}, SER^{157}, ILE^{194}, THR^{197} SER^{184}, ASP^{186}, THR^{188}, GLN^{129}, THR^{128} VAL^{164}, CYS^{178}
Active binding sites 2	ILE^{194}, GLU^{195}, ARG^{198}, THR^{197}, PHE^{201} LEU^{211}, TYR^{230}, LEU^{231}, PRO^{189}, ASP^{193} LEU^{225}, HIS^{180}, HIS^{182}, HIS^{214}, VAL^{216} VAL^{223}, SER^{224}, THR^{188}, GLY^{229},
Active binding sites 3	CYS^{134}, VAL^{164}, PHE^{165}, ALA^{168}, PHE^{176} LEU^{200}, ALA^{173}, ALA^{174}, ILE^{209}, PHE^{132} CYS^{178}, LEU^{211}, VAL^{159}, HIS^{180}, VAL^{196} HIS^{214}, ILE^{151}, THR^{197}, LEU^{225}, THR^{188} PRO^{189}, VAL^{223}, LYS^{228}, TYR^{230}

The docking calculation study revealed that residuesILE^{151}, GLY^{152}, ASN^{155}, SER^{156}, SER^{157}, VAL^{159}, HIS^{160}, PRO^{161}, GLU^{192}, GLU^{195}, VAL^{196} and ARG^{199} involved in interaction as shown in **Figure 26** and **Table 10** these residues which were important residues of major active binding site with binding energy 4.3180 Kcal/mole and dissociation constant 683697536.0 shown in **Table 10**.

Table 10: Binding energy and dissociation constant obtained during docking calculation

Cluster	Binding energy Kcal/mole	Dissociation constant[PM]	Contacting receptor residues
001	000004.3180	00000683697536.0000	ILE^{151} GLY^{152} ASN^{155} SER^{156} SER^{157} VAL^{159} HIS^{160} PRO^{161} GLU^{192} GLU^{195} VAL^{196} ARG^{199}
002	000004.2800	00000728984704.0000	ILE^{151} SER^{156} VAL^{159} HIS^{160} PRO^{161} GLU^{192} GLU^{195} VAL^{196} ARG^{199} LEU^{200}
003	000004.1320	00000935844800.0000	ILE^{151} SER^{156} VAL^{159} HIS^{160} PRO^{161} ARG^{162} GLU^{192} GLU^{195} VAL^{196} ARG^{199} LEU^{200}
004	000004.0980	00000991119872.0000	THR^{128} GLN^{129} HIS^{131} VAL^{133} LEU^{135} LYS^{146} THR^{148} VAL^{179} HIS^{180} ASN^{181} ILE^{217}
005	000004.0760	00001028613888.0000	GLU^{130} HIS^{182} PRO^{183} SER^{184} ASP^{186} THR^{188} SER^{190} GLU^{192} ASP^{193}
006	000003.9780	00001213632896.0000	THR^{128} GLN^{129} GLU^{130} HIS^{182} PRO^{183} SER^{184} THR^{188} SER^{190} GLU^{192}
007	000003.9710	00001228056704.0000	THR^{128} GLN^{129} HIS^{131} VAL^{133} LEU^{135} LYS^{146} THR^{148} VAL^{179} HIS^{180} ASN^{181} ILE^{217}
008	000003.8410	00001529359744.0000	HIS^{160} PRO^{161} ARG^{162} PHE^{165} LYS^{166} PHE^{169} ARG^{199} CYS^{203} LEU^{206} ILE^{207}
009	000003.7970	00001647259776.0000	THR^{128} GLN^{129} HIS^{131} VAL^{133} THR^{148} VAL^{179} ASN^{181} HIS^{182} PRO^{183} ILE^{217} GLY^{218} ASP^{219}
010	000003.7890	00001669652864.0000	HIS^{160} PRO^{161} ARG^{162} PHE^{165} ARG^{199} CYS^{203} LEU^{206} ILE^{207}
011	000003.7460	00001795335424.0000	THR^{128} GLN^{129} HIS^{131} VAL^{133} VAL^{179} HIS^{180} ASN^{181} HIS^{182} PRO^{183} ILE^{217} ASP^{219}
012	000003.5840	00002359897600.0000	THR^{128} HIS^{131} VAL^{133} LEU^{135} LYS^{146} THR^{148} VAL^{179} HIS^{180} ASN^{181} ILE^{217}

Docking calculation and residuals interaction confirmed that the hypothetical protein (NP_390682.1) may involve in Malathion biodegradation. **Figure 26** shows (a) protein (NP_390682.1) docking details with Malathion and (b) major active site and (c) 2D residual interaction involved for Malathion biodegradation by *Bacillus* sp. S_4.

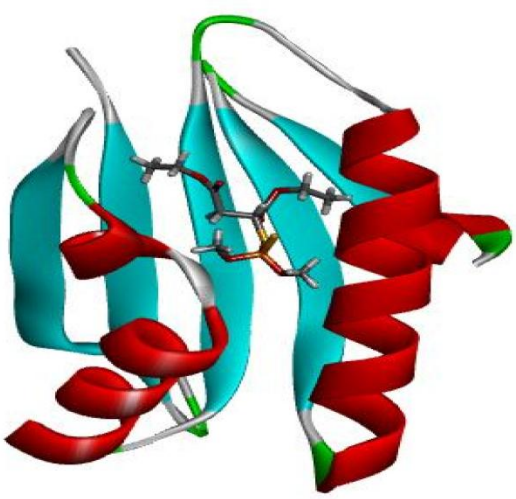

(a) Protein (NP_390682.1) docking

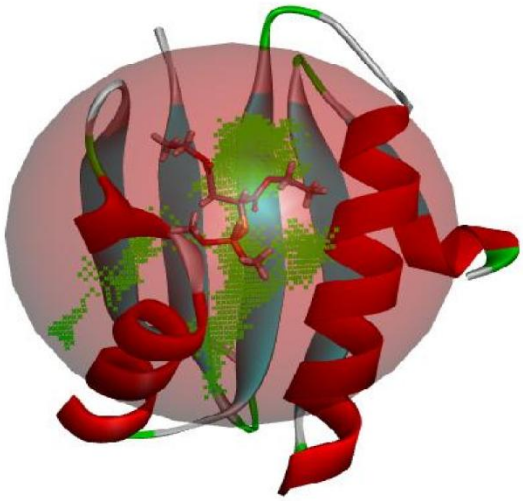

(b) Major active sites of protein

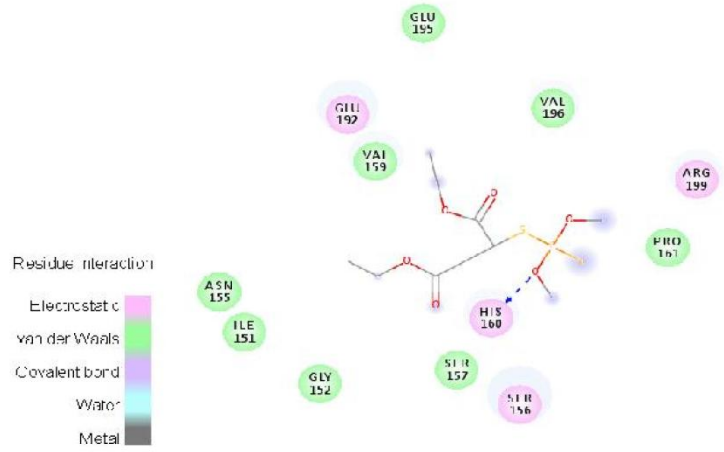

(c) 2D-residual interaction with malathion

Figure 26: Shows (a) protein (NP_390682.1) docking with Malathion and (b) major active sites of dock protein with Malathion (c) 2D-residual interaction with Malathion

Section B: Treatment of mixtures of pesticide

4.12 Experimental study for mixed pesticides: Startup and performance of IATP

Performance of aerobic plant (**Fig 27**) was evaluated using isolated microorganisms for 30 days by changing the operating conditions. Microorganisms were cultured in reactor-1 using a 100 g/L of glucose solution , MSM and trace elements over a duration of 240 hrs. Tang and You (2012) reported that the *Bacillus* sp. break down triazophos present sewage sludge wastewater by metabolization using nutrients such as peptone, yeast extract, and glucose.In the startup period, complete biodegradation of glucose is carried out in reactor-1 with stable biomass with constant pH (neutal). At the end of start-up period, the synthetic wastewater (**Table 11**) which was measured to have a COD of 1232 mg/L, was sent in to the reactor-1 with a flowrate of 2.5 l/hr. COD (in mg/L) of discharge solutions of reactor-1 and reactor-2 were recorded at a constant time period of 12 hrs. **Figure 27** represents the change in pH, DO, Redox and BOD5/COD with respect to percntage COD removal with operation time reactor-1. The overall performance of percent COD removal with time was evaluated to observe that COD removal was decreasing with respect to time.

This may be due to two particular conditions, the first of which is the fixed intervals of feed supply (2 hrs feed supply while remaining 10 hrs of operation per day) of wastewater sent to reactor-1 and second being inadequate biomass to control the increase of % COD removal. The results are in agreement with previously reported studies of (Celis *et al*., 2008; Li *et al*., 2014). Li *et al*. (2014) stated that decrease in % COD removal of effluent consisting pesticide due to bounded availability of pesticide for culturing of microorganisms.

Table 11: Physico-chemical characteristics of the wastewater

Parameter	Wastewater sample	
	Before treatment	After treatment
Nitrate (ppm)	1.227	-
Sulfate (ppm)	4.265	-
Phosphate (ppm)	4.073	-
Fluoride (ppm)	0.890	0.270
Chloride (ppm)	51.906	0.461
Bromide (ppm)	0.295	-
Calcium (ppm)	111.811	10.211
Magnesium (ppm)	40.364	2.571
Sodium (ppm)	65.706	6.461
Potassium (ppm)	18.492	0.267
Lithium (ppm)	0.089	-
TDS (ppm)	224.7	391.6

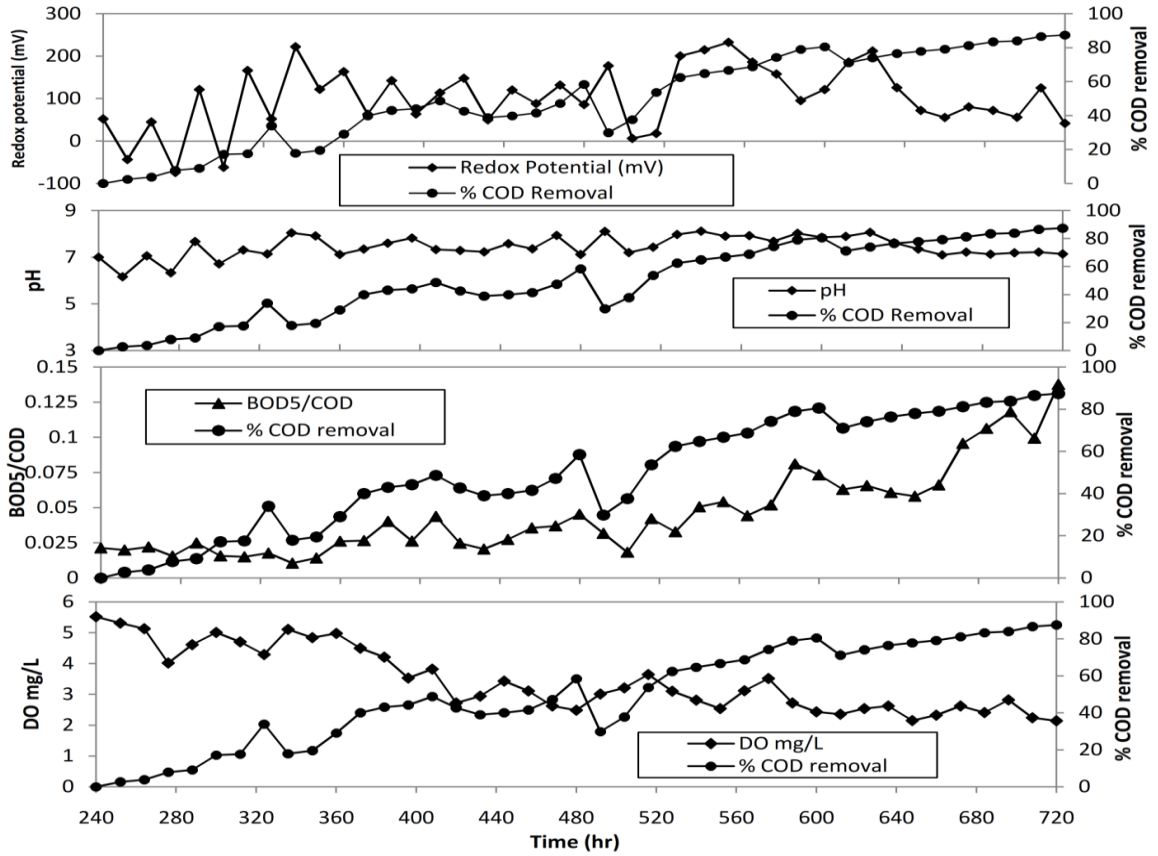

Figure 27: Performance of IATP evaluated using operating parameter such as pH, DO, Redox and BOD_5/COD.

Irregularities in % COD removal were found on 336th, 420th, 492nd and 612th hr of working time. To suppress this deviations in COD removal, pH and aeration flow rate of reactor-1 was optimized to maintain biomass concentration to increase performance of aerobic treatment plant. **Figure 28** shows % COD removal of reactor-1 where 87.5% of COD removal was recorded on the 30th day of experimentation. **Table 12** shows retention time (RT) of 72 hrs. Cesar and Ros (2013) stated that retention time plays a important role in biodegradation process whereas in the present report retention time has been maintained at 72 hrs. Li *et al*. (2014) reported that effective removal of sludge and organic pollutants has been carried out in Pilot Scale Continous Aerobic Anaerobic Coupled Reactor (CAAC).

The operating conditions such as pH, Dissolved Oxygen, Redox and BOD5/COD were varied and inspected with respect to % COD removal. pH is changed from 6.16 to 8.11 while DO is changed from 2.14 mg/L to 5.52 mg/L and Redox is changed from -74 to 232.5 mV.

pH plays vital role in degradation of organic pollutants. Russell and Dombrowski (1980) reported that reduction in biomass yield corresponds to lowering pH less than 7. Cycon *et al.* (2009) studied that highest bacteria growth was at a pH of 7±1 for degradation of diazion in soil for pseudomonas species.In the present study, firstly the wastewater with pH 7 was sent to reactor-1 and pH was measured at constant time period of 12 hrs. The results observed were similar to studies reported by (Cycon *et al.*, 2009; Yadav *et al.*, 2014) where pH deviates within the range of 7±1 approximately and interactions among pH and % COD removal as no significance

The changes in dissolved oxygen with time was evaluated and shown in **Figure 28.** Intially dissolved oxygen was 5.52 mg/L in reactor-1. On further treatment decreasing trends

Table 12: Characteristics and performance of integrated aerobic treatment plant

Performance Parameters	**Aerobic treatment plant**	
	Reactor-1	**Reactor-2**
Reactor Volume (L)	30	30
Feed flow rate (L/h)	1.5	-
Recycle pumping rate(L/h)	-	6
Speed of agitator (RPM)	160	1
Retention time (h)	72	-
Total pollutant treated (L)	200	200
COD (mg/L)	154 to 1232	101 to 1011
BOD (mg/L)	10.6 to 28.2	-
DO (mg/L)	2.14 to 5.52	-
BOD/COD ratio	0.010485 to 0.137662	-
Ph	6.16 to 8.11	-
Redox potential	(-74) to 232.5	-
Temperature (°C)	Room temperature	Room temperature
Operation time (day)	30	30
Removal Efficiency (RE) %	87.5	91.80
% Transmission	-	46 to 73

with deviations were observed. Final DO was found to be 2.14 mg/L on 30th day (termination of operation).

Reduction in DO with respect to time is due to a increase in % COD removal because of the high rate of oxygen is increased the dissolved oxygen concentration in wastewater which is helpful for bacterial growth. As bacterial growth is increased the substrate utilization also increased (in terms of the COD value decreased). Final COD of treated wastewater in reactor-1 was reduced to 154 mg/L from an intial COD of 1232 mg/L at the end of operation (720 hrs).

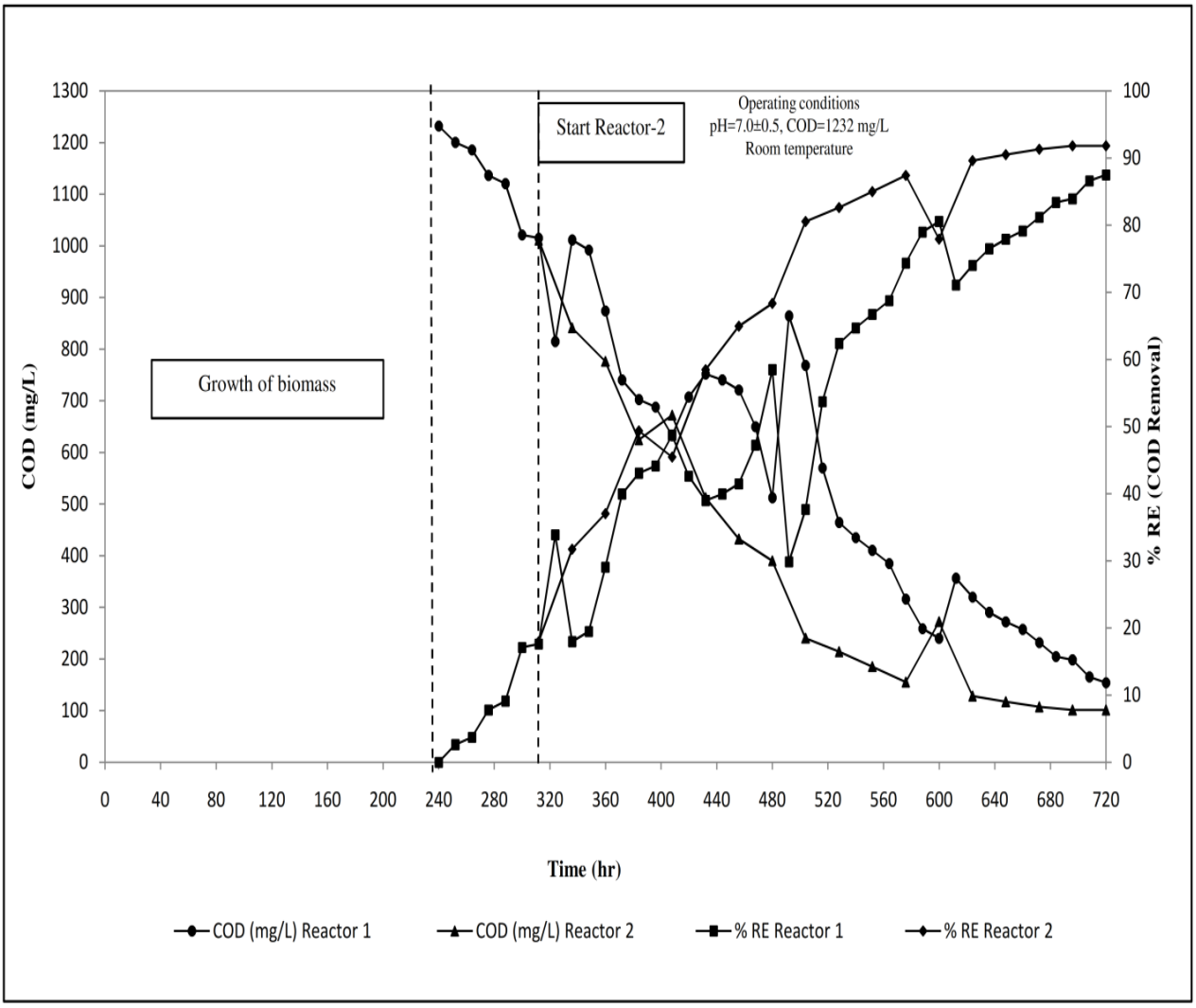

Figure 28: Overall Performance of Two Stage Integrated Aerobic Treatment Plant during the treatment of synthetic wastewater

Similar results were shown by Lim *et al*. (2014). High DO in the reactor may lead to improved removal of pollutant due to periodic aeration (Lim *et al.*, 2014; Hanhan *et al*., 2011).

Redox capacity on the biodegradation of pesticides is shown in **Figure 28**. The positive values of Redox capacity represents the degradation of pesticides using microorganisms (Pett-Ridge and Firestone, 2005). During the first stage, Redox capacity deviated from negative to positive value which supports decrease in % COD removal. At the end of 300 hrs,

Redox Potential is observed to be positive and deviated (6.3-232.5 mV) as indicated in **Figure 28**. During this stage, % COD removal increases and attains 87.5% until the pocess is terminated. Fulazzaky *et al*. (2015) reported that Redox potential varied from 44-135 mV while treating Municipal effluent in alternating aerobic anoxic reactor. Aerobic microbes like Actinomyces sp. or Azotobacter sp. are needed for high redox potential was reported by Rabotnova and Schwartz (1962). Pett-Ridge and Firestone (2005) reported that regular deviations of Redox is due to strong selective force on the phylogenetic microbial cultures and enhances metabolic redox tolerance mechanisms. Bellucci *et al*. (2011) reported lab scale aerobic anaerobic reactor is operated in the presence of oxygen limiting condition at sludge RT of 15 days, which results in mean DO of 0.63 mg/L although total nitrification occurs at minimium dissolved oxygen level with perodic aeration.

Annabi *et al*. (2016) reported that BOD5/COD ratio is used to indicate biodegradation. Further, Kumar *et al*. (2010) reported that when BOD5/COD ratio increases biodegradation in bioreactor is eminent. Minimium values of BOD5/COD represents high organic loading. During early stages, BOD5/COD ratio in reactor-1 was measured to be 0.021 that deviates as biodegradation is carried out. **Figure 27** shows increasing trends of BOD5/COD ratio with respect to % COD removal. Highest value of 0.137 is observed at the termination of operation (**Fig 27**).

An increase in the value from 0.021 to 0.137 is an representation of effective bacteria culture that easily degrades a mixture of pesticides. Similar studies are reported by Affam *et al*. (2014) in treatment of effluent consisting of pesticide in a single batch reactor. While Kumar *et al.* (2010) reported that BOD5/COD ratio is in the range of 0.65-0.67 during the treatment of effluent from pulp mill industry**.**

Analysis Of Variance (ANOVA) indiacted that pH, Dissolved Oxygen, redox and BOD5/COD ratio had a significant response ($P < 0.05$) to the biodegradation of pesticides. The mean and standard deviation for operating parameters such as pH, dissolved oxygen, redox and BOD5/COD ratio was measured to be 7.44 and 0.46, 3.44 and 1.03, 102.73 and 74.78, 0.045 and 0.030 respectively. Similar results were showed by differnt researchers for chloropyrifos and malathion ($P< 0.05$) (Yadav *et al*., 2014; Geed *et al*., 2017).

Treated wastewater discharged from reactor-1 (at the end of 36 hrs of treating) was sent into the reactor-2 for treating of raw parental pesticide and its intermediates while COD of wastewater was frequently measured. A part of treated effluent from reactor-2 was recycled at 6 L/hr to reactor-1 regularly. The slow agitation and presence of substrate lead to maximising the quantity of biomass sent to reactor-2 resulted in maximizing degradation are shown in **Figure 27 and Table 12** also increasing the overall performance of the plant. Highest % COD removal was measured to be 91.8% (**Fig. 27**) in reactor-2 at the termination of operation along with retention time of 6 hrs. Fulazzaky *et al*. (2015) stated that the performance of aerobic anaerobic plant increased to 53.4% approx. with respect to anoxic time (Retension Time; reactor-2) from 3 to 6 hrs. In reactor-2, % COD removal was increased from 87.5% (reactor-1) to 91.8% because of perodic growth of sludge. Further, steady and stable % COD removal was seen in the range of 640 hrs to 720 hrs represents the saturation of biodegradation capacity in reactor-2. Liu *et al*. (2015) reported similar type of trend during the treatment of slaughter house effluent. Lim *et al*. (2014) mentioned a 90% COD removal in Palm Oil Mill wastewater treated efficiently in a SBR. In the present study, better % COD removal than previously reported studies (Kumar *et al*., 2010; Othman *et al*.,

2013; Zhang *et al*., 2013) using aerobic bioreactors for treating livestock effluent along with digested piggery effluent.

4.13 Intermediates/ Metabolites confirmation: GC-MS

Concentration of mixture of pesticides is measured using HPLC analysis. The Control samples of mixture of pesticides untreated was measured independently and observed peaks which represent parathion, Malathion and atrazine at 1.86, 2.40 and 2.65 min RT respectively (**Fig. 29**). Similarly, HPLC analysis was carried out on treated samples of wastewater and observed Parathion, Malathion and Atrazine at 1.85 min, 2.33 min and 2.59 min respectively. Various other peaks were also observed which represents metabolites and intermediates formed at the time of degradation (**Fig 30**).

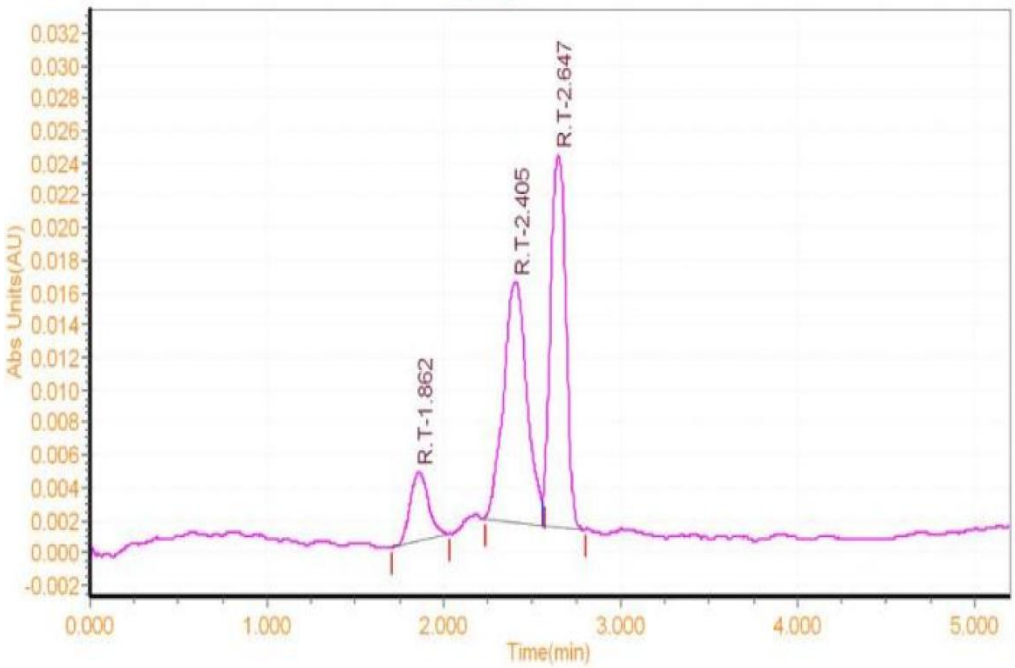

Figure 29: HPLC analysis result of mixtures of pesticide before treatment

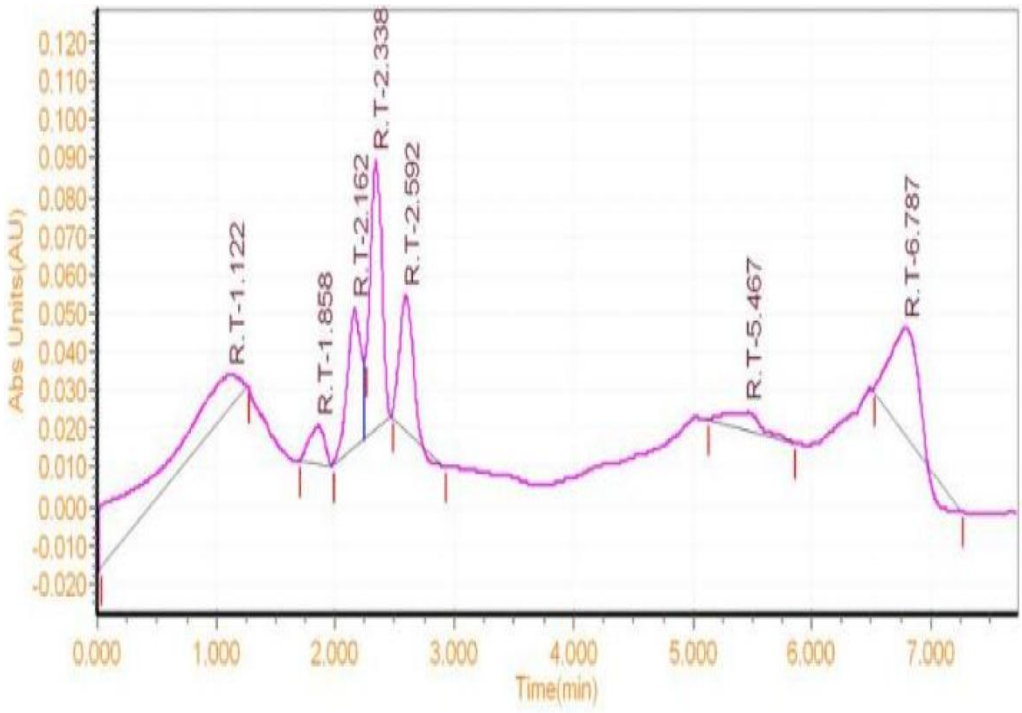

Figure 30: HPLC analysis result of mixtures of pesticide after the treatment

Wastewater sample from reactor-2 were analyzed with the help of Gas Chromatography-Mass Spectroscopy which helps in representing metabolites and successful degradation of effluent. The GC-MS results represented parental compounds along with intermediates are shown in **Figure 31** and **Table 13**. The Atrazine, Malathion, Paraathion peaks was observed during RT of 28.87 min, 32.99 min and 33.61 min respectively. A total of 3 metabolites were formed corresponding to 3 parental compounds. Atrazine corresponding metabolite was recognized as biuret observed during 11.17 min RT. Malathion corresponding metabolite was recognized as succinic acid observed during 13.55 min RT. Parathion corresponding metabolite was recognized as dithiodiphosphoric acid tetraethyl ester observed during 26.82 min RT. The results apparently showed that the metabolite of the pesticides are less toxic in nature which is advantageous during biodegradation.

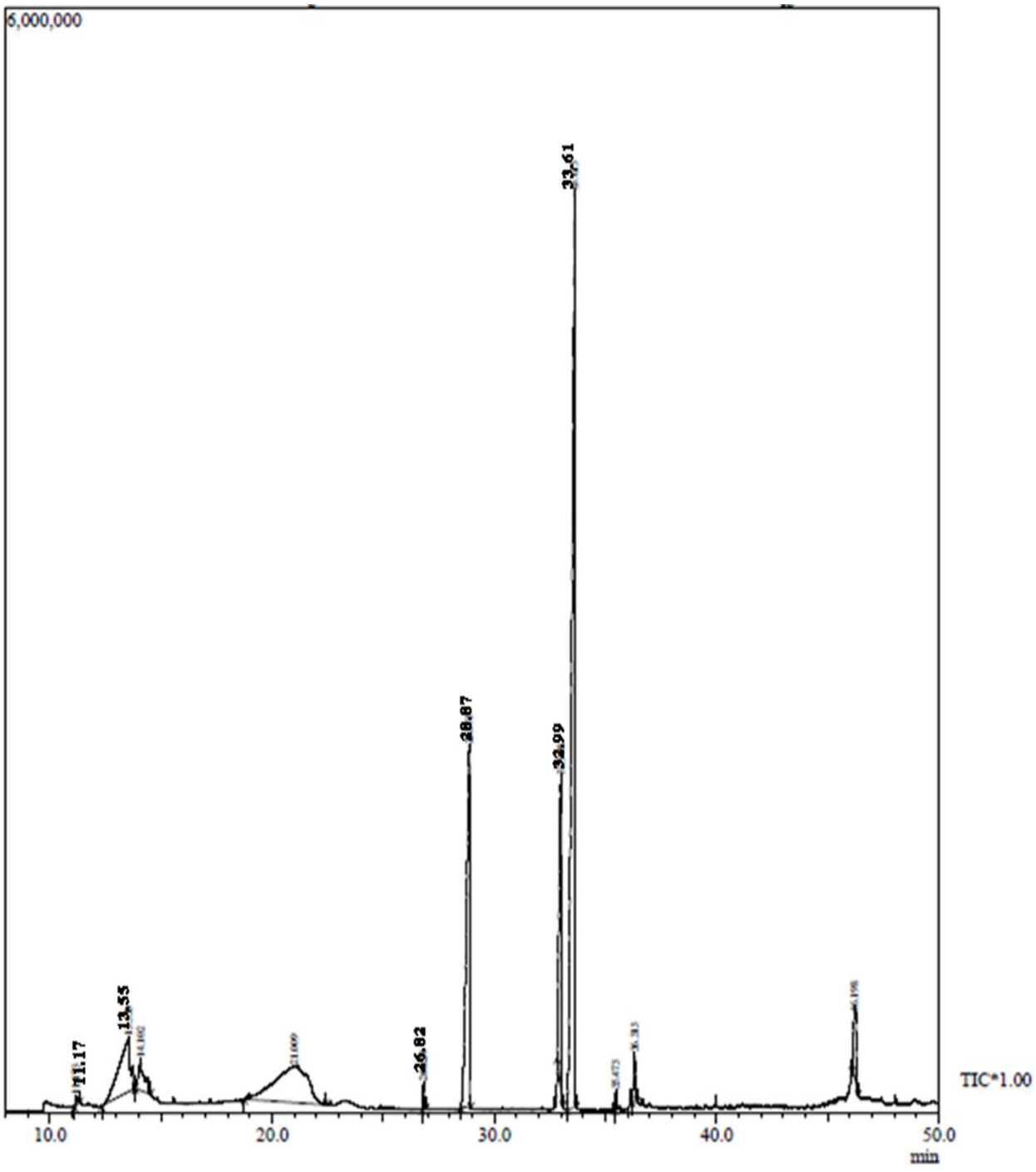

Figure 31: GC-MS analysis of effluent from Reactor-2 after the treatment of 30th days.

Table 13: Properties of parental pesticide and identified metabolites by GC-MS analysis

Compound	Chemical formulae	Half life in water	Molecular weight	Toxicity	Residence time (min)	Fragmented result of GC-MS m/z ion peak	Ref
Atrazine	$C_8H_{14}ClN_5$	>200 days.	215	Highly toxic	28.87	43,58,71,92,104,132, 158,173,187,200,218	Fang et al., 2015; Douglass et al., 2014
Malathion	$C_{10}H_{19}O_6PS_2$	2 to 18 days	330	Highly toxic	32.99	55,63,79,93,99,125,1 43,158,173,211, 256,285	Geed et al., 2017
Parathion	$C_{10}H_{14}NO_5PS$	2 to 10 day	291	Highly toxic	33.61	29,97,109,137,155,18 6,218,235,263,291	Zhao and Hwang, 2009
Biuret	$C_2H_5N_3O_2$	9 to 10 days	103	Less toxic	11.17	42, 44, 59, 70, 102	Fang et al., 2015;Douglas et al., 2014
Succinic acid monomethyl ester	$C_5H_8O_4$	5 to 7 days	132	Less toxic	13.55	55, 59, 73, 83,101, 114	Geed et al., 2017;WHO, 2015
Dithiodiphosphoric acid tetraethyl ester	$C_8H_{20}O_5P_2S_2$	-	322	Less toxic	26.82	65,97,121,145,174,19 3,202,210,238,266,29 4,322	Zhao and Hwang, 2009;WHO, 2015

Various researches have shown identical reports for GC-MS analysis of atrazine, malathion and parathion degradation (Zhao and Hwang, 2009; Fang *et al*., 2015; Geed *et al*., 2017). Biodegradation of insecticides is an chain of enzyme activated reaction where two intermediates are produced which are stable and unstable subjected to the type of enzyme produced by microbes to metabolize the insecticides (Zhao and Hwang, 2009). Fang *et al*. (2015) reported that atrazine biodegradation route with thorough knowledge regrading intermediates produced at the time of biodegradation. Atrazine chloro hydrolase plays important role in degradation of atrazine. It transforms atrazine to hydroxyatrazine that is further degraded to cyanuric acid and biuret by catalase enzyme.The reported metabolite biuret is less toxic than atrazine (Fang *et al*., 2015; Douglass *et al*., 2014). The detected metabolite succinic acid mono-methyl ester was produced due to malathion metabolism. Succinic acid mono-methyl esterase enzyme is the sole reason for malathion firstly converted to succinic acid mono-methyl ester and finally to succinate with a chain of enzyme assited reactions (WHO, 2015; Geed *et al*., 2017). Zhao and Hwang. (2009) reported similar type of results where parathion was degraded to form intermidiates recognised as dithiodiphosphoric acid tetraethyl ester. On further decomposition it formed ethythiophosphate and finally phospahte is formed using various enzyme catalyzed reactions.Various studies showed that the hydrolysis of ester bond is a routine biodegradation stage in organic compounds containing phosphorous this is not likely to be pronounced as vital mechanism because P-S bonds were still intact (Zhao and Hwang, 2009). Pesticides biodegradation is carried out using oxidase enzyme, hydrolase enzyme or complex mixture of oxidase and hydrolase (Geed *et al*., 2017; Yadav *et al*., 2014).

4.14 Biodegradation kinetics and evaluation of death phase

Designing and scale up of proposed plant was carried out with the help of substrate utilization kinetics (Affam *et al*., 2014). In the present study, Monod growth kinetics was evaluated to fit with experimental values and kinetics was evaluated with the use of equation (5). The First order rate constant (*Kobs*) was calculated to be 0.00425/hr (0.102/day) as represented in **Figure 32 (a)**. Affam *et al*. (2014) reported that the value of *Kobs* is 0.01332/hr during the treatment of effluent comprising of pesticides in a SBR. The kinetics gives specific details regarding cell history, the microorganism's intrinsic characteristics and present environmental conditions (Beltran-Heredia *et al*., 2000).

Cell Yield value ($Y_{x/c}$) and Biomass Decay value (K_{dp}) are extremely vital kinetic parameters regarding the estimation of biomass concentration over the course of the aerobic treatment plant (Beltran-Heredia *et al*., 2000; Martin *et al*., 2008). The $Y_{x/c}$ indicates amount of biomass formed per amount of substrate used and K_{dp} represents the significance of endogenous metabolism into a cell culture (Beltran-Heredia *et al*., 2000). During the course of operation of treatment plant, the concentration of biomass may decrease because of the presence of toxic pollutants/metabolite produced. For the growth cycle of bacterial culture, the death phase is considered when there is a decrease in the count of bacterial cells. Bailey and Ollis (1986) reported that the relative calculations have been carried out in this phase, due to various industrial microorganisms processes are stopped ahead of the death phase.. The value of *Yx/c* and K_{dp} were caluclated from a plot of μ *vs.* q represented in **Figure 32 (b)**. The values of $Y_{x/c}$ and K_{dp} was found to be 0.696 mg COD/mg MLSS (Mixed Liquor Suspended Solids) and 0.0010/hr, respectively. Similar results were reported Affam *et al*.(2014) and Martin *et al*. (2008) showed that $Y_{x/c}$ 0.5301 and 0.5 and K_{dp} 0.0072 and

0.004/hr respectively for the degradation of pesticides in effluent. Beltran-Heredia *et al*. (2000) showed values of $Y_{x/c}$ 0.227 and K_{dp} 0.0069/hr for the degradation of black olive effluent which was confirmed by the biomass concentration. Both exponential growth and death phase have been studied for the kinetic study for estimating the first order rate constant *Kobs*, *Yx/c* and K_{dp} which is useful for the metabolism of bacterial species used in wastwater treatment process.

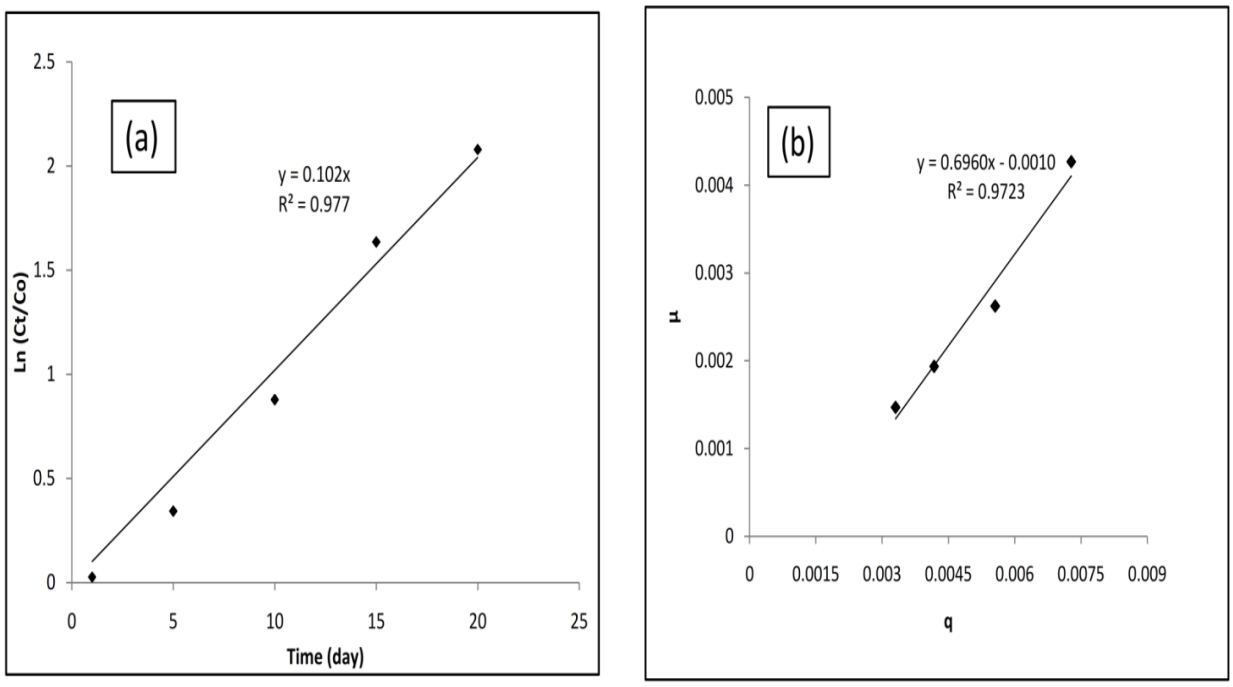

Figure 32: Kinetic study for (a) estimation of first order rate constant (K_{obs}) and (b) Cell Yield ($Y_{X/C}$) and Decay Coefficients (K_{dp}).

Section C: Hybrid reactor for atrazine removal

4.15 Parametric optimization: UV Fenton

The effect of H_2O_2/COD molar ratio on % removal of atrazine was studied by varying H_2O_2/COD molar ratio. The % removal was found to be 55, 52 and 68% for H_2O_2/COD molar ratio of 0.25, 0.5 and 0.75 respectively. The H_2O_2/COD molar ratio was increased from 1 to 1.5, and corresponding % removal decreased from 62% to 52%. The maximum removal was 68% at H_2O_2/COD molar ratio 0.75 (**Fig 33**). It was observed that the H_2O_2/COD molar ratio 0.75 was optimum for degradation of Atrazine. The possible reason behind decreased removal efficiency of atrazine is excess of H_2O_2, after addition, that scavenges OH*.

$$OH^* + H_2O_2 \longrightarrow H_2O + HO_2 \qquad (17)$$

Increasing H_2O_2/Fe^{2+} molar ratio from 5 to 25 increased the degradation of Atrazine, but there was a decrease in degradation for H_2O_2/Fe^{2+} molar ratio 25 to 50. The maximum removal was 62% at H_2O_2/Fe^{2+} molar ratios of 25 as shown in **Figure 33**. The decrease in the degradation of Atrazine at increased Fe^{2+} concentration was presumably due to direct reaction of OH^* radical with Fe^{2+} at high concentration as in reaction (Joseph *et al*., 2000).

$$Fe^{2+} + OH^* \longrightarrow Fe^{3+} + OH^- \qquad (18)$$

When pH increased from 1 to 2.5, Atrazine removal was increased up to 60%, but beyond pH 2.5, removal decreased as shown in **Figure 33**. The maximum removal was observed at pH 2.5.

The further experiments were conducted at optimum operating conditions. The ANOVA analysis results show that H_2O_2/COD, H_2O_2 /Fe^{2+} and pH had a significant effect ($P<0.05$) on the % removal of Atrazine.

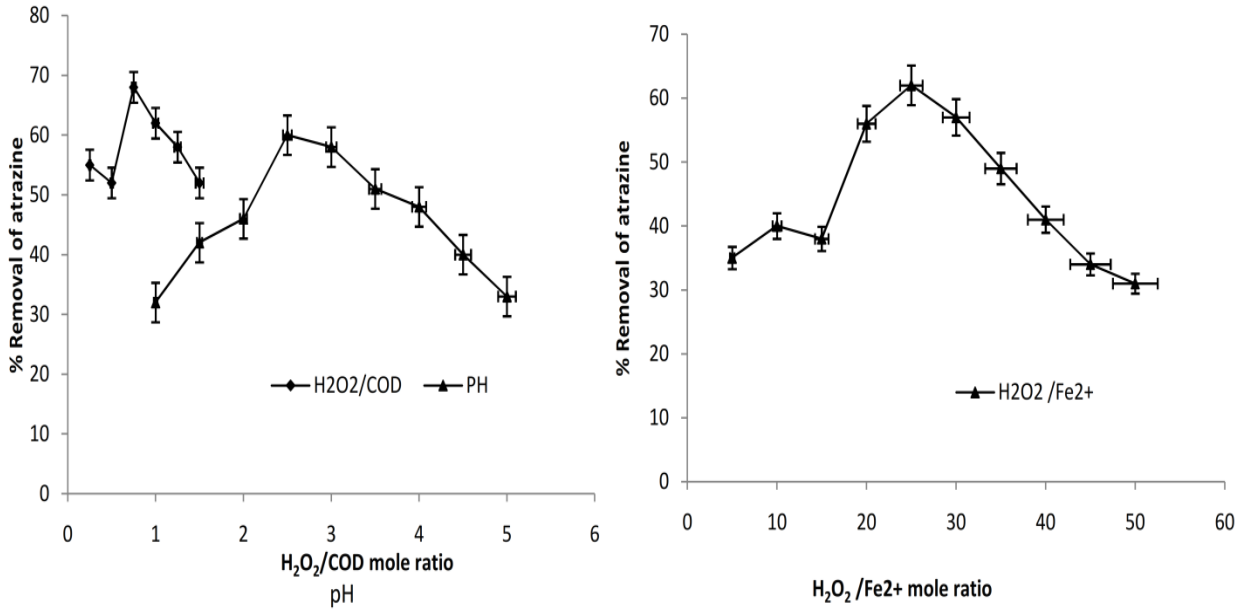

Figure 33: Parameter optimization in UV-Fenton process

4.16 Parametric optimization: bioreactor

The parameters for bioreactor were optimized by varying one parameter and keeping all other parameters fixed. The effects of pH and DO for the removal of Atrazine were investigated at constant Atrazine concentration 150 mg/L as shown in **Figure 34**. The experiments were conducted at pH range (4.0-9.0) and DO (3.5-7.5). The effects were studied, and maximum removal of 69 % was found at pH 7.0. At alkaline pH, there was a decrease in Atrazine degradation rate which is similar to the observation of Singh *et al.* (2003) who reported the inhibitory effect of pH in the alkaline range (pH>8) on the metabolism of microorganisms. The effect of DO level was studied, and a maximum removal

of 68 % was observed at DO 6.0 mg/L. DO level is a very important parameter for consumption or utilization of substrates at high loading rate. As low DO level in bioreactor results in low oxygen concentration, which may be the reason for the decrease in growth of microbes and removal of Atrazine (Mohan *et al*., 2006). The findings were similar to the results obtained by Mohan *et al*. (2006). The ANOVA analysis shows that the pH and DO had a significant effect ($P < 0.05$) on the removal of Atrazine. The present result was in line with results obtained by various researchers for other pollutants (Tazdait *et al*., 2013; Geed *et al*., 2017).

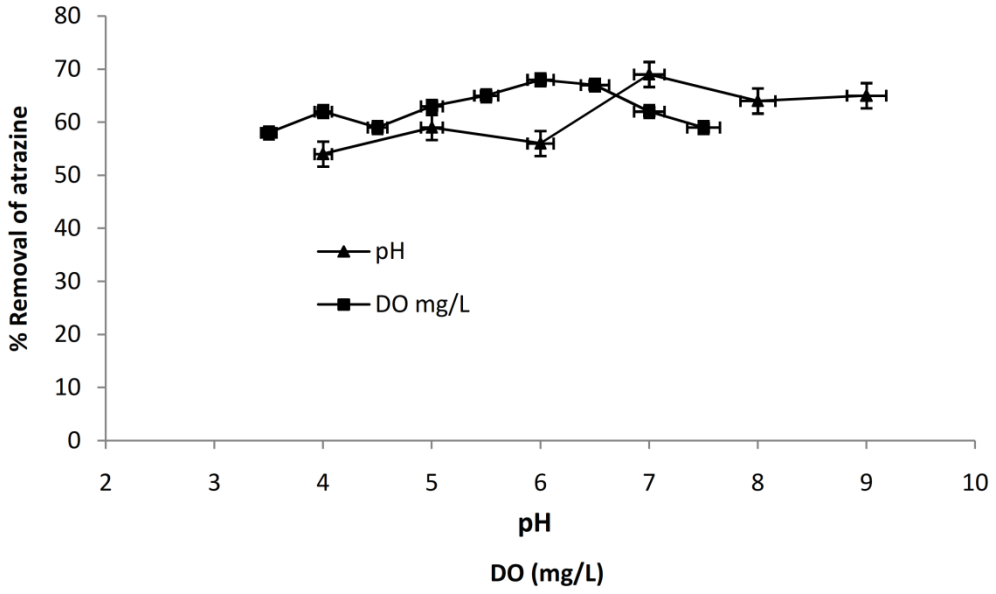

Figure 34: Parameter optimization in packed bed bioreactor

4.17 Performance evaluation of coupled process: UV Fenton and bioreactor

The experiments were performed with combined treatment plant (three stages) including UV-Fenton (advanced oxidation process), pH neutralization (stabilization) and biodegradation process. In the stage-I (UV-Fenton process), the experiments were carried out at 300 mg/L of Atrazine at optimum process parameters pH, molar ratios of H_2O_2/COD and

$H_2O_2/Fe^{2+}$and room temperature. The removal of Atrazine was found to be 65 % in 60 minutes which was indicated by a reduction in concentration upto 100 mg/L (**Fig. 35**). Garza-Campos *et al*. (2017) reported that 65% removal of Atrazine concentration at 20 mg/L. In the present study, the maximum removal of Atrazine at 300 mg/L by Fenton reactor was 65% in 60 min as shown in **Figure 35**. Affam *et al.* (2014) also reported a maximum removal of 64.8 % at H_2O_2/COD molar ratio 2, H_2O_2/Fe^{2+} molar ratio 25 and pH 3.

In phase-II, the effluent from UV-Fenton process was transferred through filtration unit (0.2 µm). The pH was adjusted (by HCl/NaOH) to nearly neutral (7±0.2) with holding time 60 min and fed to the bioreactor in phase-III for the microbial treatment. pH is considered as one of the most important parameters for affecting the degradation of Atrazine while applying advanced oxidation processes like UV Fenton, Photo-Fenton etc.(Grcic *et al*., 2009; Debasmita *et al*., 2013).

In phase-III, after the immobilization (15 days), the Atrazine was treated in the bioreactor. The bacterial sp. immobilized on Loofa was used for treatment. The lower concentration of Atrazine (100 mg/L) was transferred to bioreactor phase-III next to phase-II. Several researchers have reported the bio-treatment of Atrazine is favored at lower concentration (Debasmita *et al*., 2013; Douglass *et al*., 2015; Zhang *et al*., 2017). Biodegradation of Atrazine was conducted in bioreactor and Atrazine concentration was monitored day to day during the operation. The removal efficiency enhanced from 65 % to 93 % in continuation with the Fenton reactor during 12 days of operation excluding immobilization period. The performance of coupling method was studied as shown in **Figure 35** Atrazine degradation was carried out at pH 7.0±0.2 in a bioreactor using mixed consortia immobilized on Loofa. Atrazine removal increased upto 74% on the 3rd day of operation and

corresponding Atrazine concentration was achieved 78 mg/L. On 4th day slightly decrease in % removal was observed which may be due to substrate deficiency; the formation of fouling which causes the oxygen limitation as reported by Kureel *et al.* (2016) and Geed *et al*. (2016) Removal efficiency increased again upto 93% on the9th day of operation. Further, it became constant to 93% upto 12th day with corresponding Atrazine concentration of 21 mg/L. Du *et al*. (2011) reported 74.09 % removal in 15 days and Sanchis *et al*. (2014) reported 80% Atrazine removal by coupling of Fenton and Biological oxidation processes.

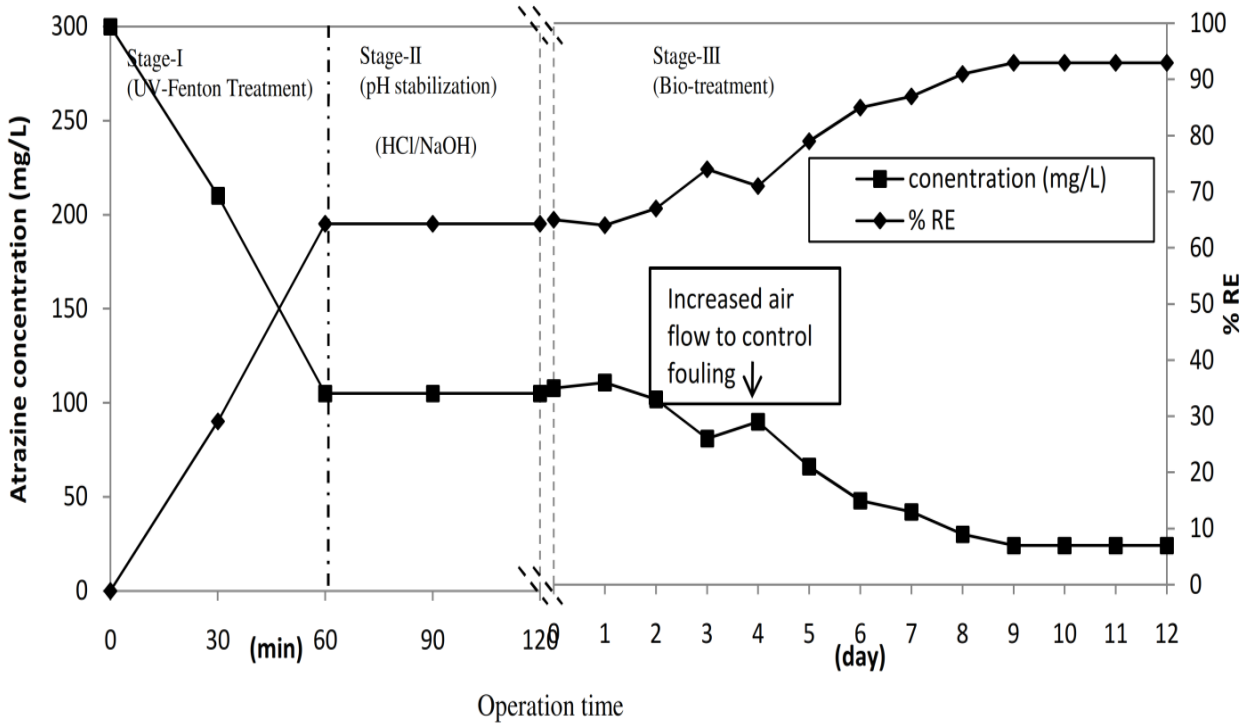

Figure 35: Three stage coupling method for the removal of Atrazine

4.18 Analysis of residual Atrazine: HPLC and GC-MS

HPLC analysis was performed to find out the concentration of Atrazine before and after the experiment. The control Atrazine sample was run separately, and the peak was found at 2.5 min time interval as shown in **Figure 36(a)**. The similar analysis was done for treated effluent sample. The Atrazine (2.5 min) and its intermediates were found at different time interval as shown in **Figure 36(b)** in treated effluent sample. Further, the intermediates were confirmed by GC-MS analysis.

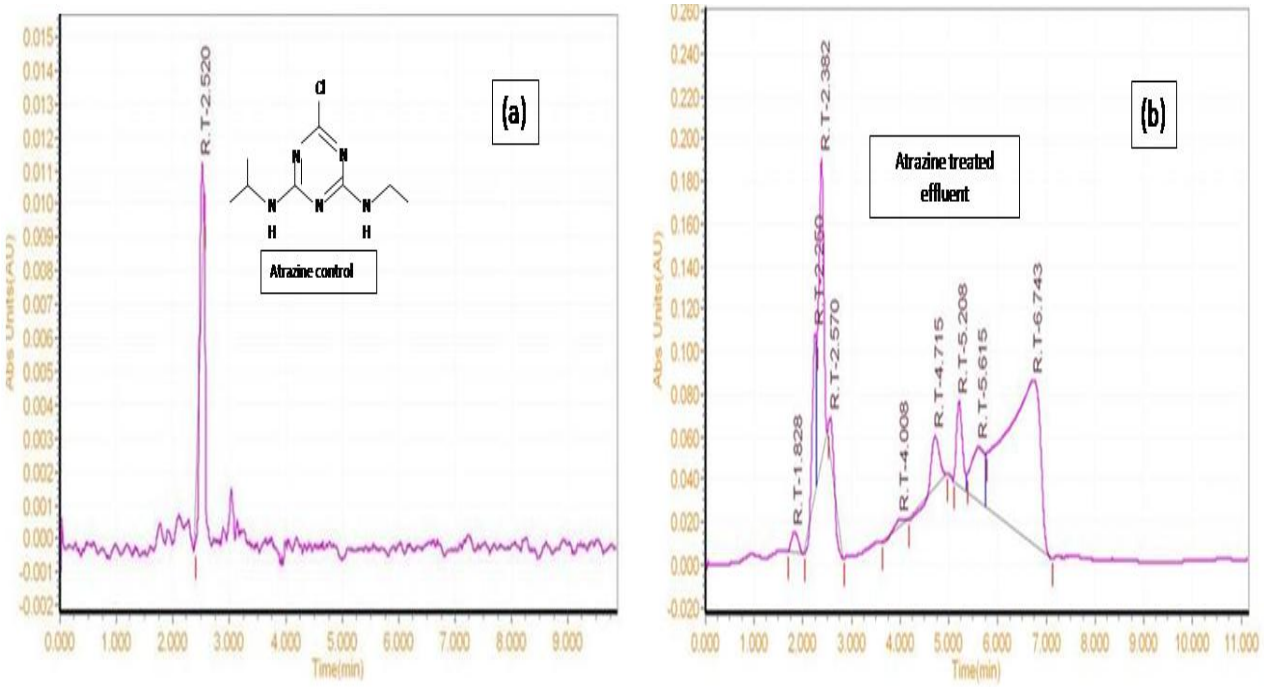

Figure 36: HPLC analysis of control (a) Atrazine and (b) effluent sample after treatment

The GC-MS analysis of control Atrazine sample and treated effluent was performed. The GC-MS fragmented pattern of Atrazine showed parent ion peak at m/z 43, 58, 92, 173, 187, 200 and 215 as shown in **Figure 37a**. The GC-MS result confirmed that the Atrazine degraded during the treatment process. The **Figure 37b** showed a fragmented pattern of biuret parent ion peak at m/z 42,44,59,70 and 102. The similar fragmented pattern for urea showed (**Fig. 37c**) m/z ion peak at and 26, 28, 44 and 60. In the present work, Atrazine was

degraded during the treatment process and converted to two metabolites (biuret and urea) as confirmed by GC-MS result, which is in agreement with previous works (Vargha *et al*., 2005; Fang *et al*., 2015). Vargha *et al*., (2005) reported that the isolated cultures were capable of utilizing Atrazine as sole carbon and nitrogen source efficiently.

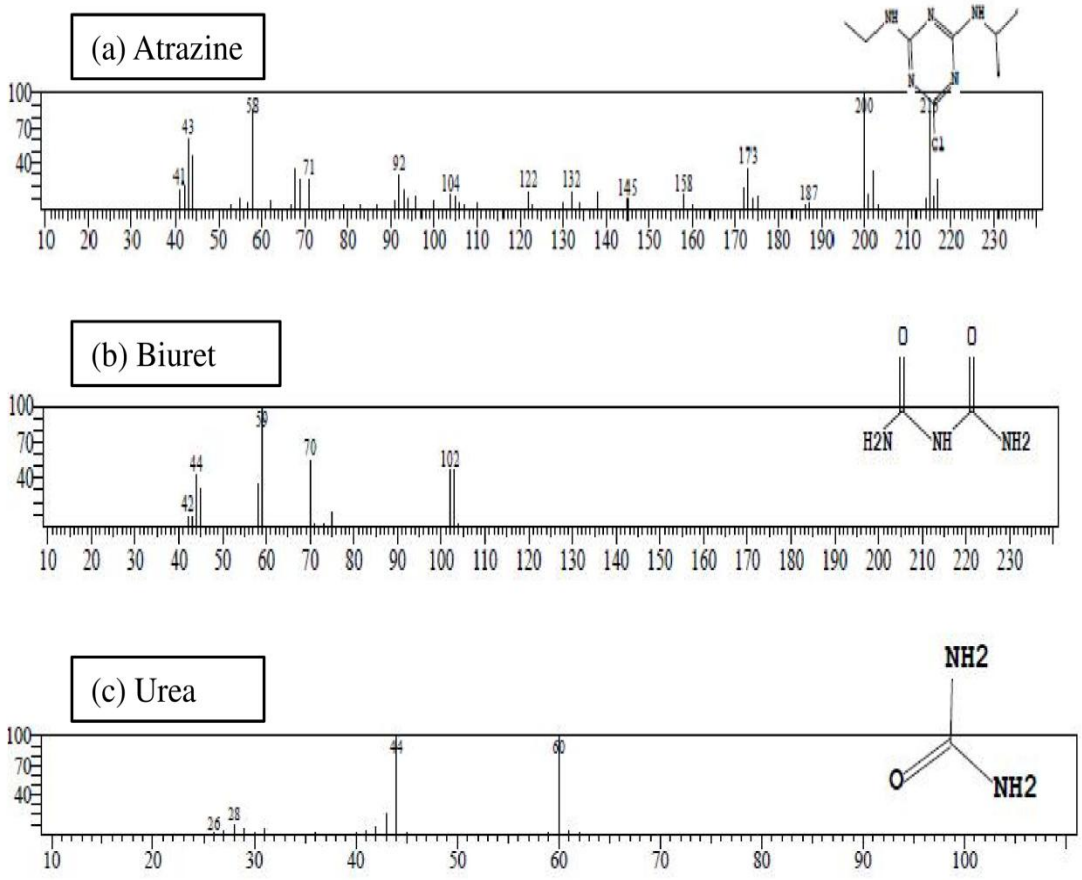

Figure 37: GC-MS analysis of control (a) Atrazine and effluent sample after treatment shows intermediates (b) Biuret and (b) Urea